Characterisation and semi-mechanistic modelling of eflornithine pharmacokinetics and evaluation of prodrugs in oral treatment against late-stage human African trypanosomiasis

Carl Johansson

Department of Pharmacology

Institute of Neuroscience and Physiology

Sahlgrenska Academy at University of Gothenburg

UNIVERSITY OF GOTHENBURG

Gothenburg 2013

Characterisation and semi-mechanistic modelling of eflornithine pharmacokinetics and evaluation of prodrugs in oral treatment against late-stage human African trypanosomiasis

carl.johansson@pharm.gu.se/c-c.johansson@telia.com

A bottle of wine contains more philosophy
than all the books in the world.
L. Pasteur

Characterisation and semi-mechanistic modelling of eflornithine pharmacokinetics and evaluation of prodrugs in oral treatment against late-stage human African trypanosomiasis

Carl Johansson

Department of Pharmacology, Institute of Neuroscience and Physiology
Sahlgrenska Academy at University of Gothenburg
Gothenburg, Sweden

ABSTRACT

The present thesis explores the hypothesis that treatment of human African trypanosomiasis can be improved by characterising the enantioselective pharmacokinetics of eflornithine, and investigating the oral eflornithine absorption. Eflornithine pharmacokinetics after oral single dose or intravenous administration in the rat was well described by a three-compartment model with saturable distribution to one peripheral, binding, compartment. Enantiospecific oral bioavailability was estimated at 32 and 59% for L- and D-eflornithine, respectively. Although eflornithine enantiomers display similar rates of absorption their extents of absorption differed. This may be caused by a chemical complex in the gut rendering less L-eflornithine available for absorption. In an attempt to improve oral bioavailability, prodrug candidates were synthesised and administered orally to the rat. The candidates were found to be metabolically too stable and did not deliver eflornithine *in vivo*. Furthermore, *in vitro* permeability, potency and metabolic stability for the prodrugs were investigated. The pharmacodynamics in man was mathematically modelled in a time-to-event approach and three different eflornithine based treatments were compared. The three-fold difference in potency between oral and intravenous eflornithine monotherapy may suggest that it is mainly the L-eflornithine enantiomer that elicits the anti-trypanosomal effect, since the oral bioavailability for the L-enantiomer is reported to be about 30% *in vivo*. Further investigation into the separate eflornithine enantiomers is motivated since the potency differs and combination with nifurtimox further improves efficacy which could enable an oral eflornithine based dosage regimen.

SAMMANFATTNING PÅ SVENSKA

Denna avhandling avser utvärdera möjligheterna kring en oral behandling mot afrikansk sömnsjuka. Sömnsjuka orsakas av en parasit av *trypanososma brucei*-släktet och smittspridningen sker via tsetseflugan (*lat. Glossina*). Eflornitin är rekommenderad förstahandsbehandling i sömnsjukans senare stadie och ges då som ett dropp fyra gånger om dagen i fjorton dagar med en dos på 100 mg per kg kroppsvikt. Detta kräver att det finns tillgång till steril utrustning, utbildad sjukvårdspersonal och en infrastruktur som klarar av att distribuera den totalt ca 30 kg per behandling tunga förpackning som behandlingen utgör. Då detta inte alltid finns att tillgå, framförallt på den afrikanska landsbyggden, betyder det att tusentals dör årligen trots att existerande behandling finns. Det vore en stor förbättring om eflornitin kunde tas oralt, då detta skulle minska kostnaden och göra behandlingen mer lättillgänglig.

Eflornitin är en kiral molekyl, vilket innebär att den förekommer som två spegelvända konformationer, L- (vänster) och D-eflornitin (höger). Tidigare undersökningar har kunnat fastslå att dessa spegelbilder uppför sig olika med avseende på effekt och hur de tas upp från tarmen in i blodet. Då detta får stor påverkan på hur en behandling utformas är behovet av en vidare utredning mycket motiverat. I denna avhandling har två möjligheter till en oral behandling undersökts, varav en är att ändra den kemiska strukturen på eflonitin och på så sätt öka upptaget i tarmen. Ett antal så kallade prodrugs har utvärderats med avseende på ökat upptag i tarmen på råtta. Principen är att kemiska grupper som fästs på eflornitinmolekylen skall klyvas bort av kroppens enzymer efter upptaget i tarmen. Dock visade det sig att de undersökta substanserna hade mycket hög stabilitet och inte bioaktiverades, vilket medförde att den önskat ökade parasitavdödande effekten förväntas utebli.

Den andra delen av avhandlingen fokuserar på att förstå skillnaden mellan L- och D-eflorntin framför allt upptaget i tarmen och fördelningen i kroppen. En skillnad mellan L och D har påvisats i absorptionen där L-eflornitin absorberas till hälften av D-eflornitin. Den bakomliggande mekanismen till skillnaden i upptag i tarmen har föreslagits bero på en komplexbildning vilket hämmar upptaget av L- eflornitin. Denna avhandling stödjer också tidigare rapporter att L-efornitin verkar mer aktiv än D-eflornitin, en skillnad som får stor betydelse för möjligheterna att designa en oral behandling. Det finns enbart begränsat med tidigare rapporter angående skillnaderna mellan L och D-eflornitin och denna avhandling stödjer en fortsatt undersökning för att eventuellt möjliggöra en oral behandling mot det sena stadiet av afrikansk sömnsjuka.

LIST OF PAPERS

This thesis is based on the following studies, referred to in the text by their roman numerals.

I. Cloete TT, **Johansson CC**, N'Da DD, Vodnala SK, Rottenberg ME, Breytenbach JC, Ashton M. Mono-, di- and trisubstituted derivatives of eflornithine: synthesis for *in vivo* delivery of DL-alpha-difluoromethylornithine in plasma. *Arzneimittelforschung*. 2011;61(5):317-25.

II. **Johansson CC**, Cloete TT, N'Da DD, Breytenbach JC, Svensson R, Jansson-Löfmark R, Ashton M. *In vitro* and *In vivo* Pharmacokinetic Evaluation of Eflornithine Based Prodrugs for Oral Treatment of Human African Trypanosomiasis. (*Submitted*)

III. **Johansson CC**, Gennemark P, Artursson P, Äbelö A, Ashton M, Jansson-Löfmark R. Population pharmacokinetic modeling and deconvolution of enantioselective absorption of eflornithine in the rat. *Journal of pharmacokinetics and pharmacodynamics* 2013;40(1):117–128

IV. **Johansson CC**, Ashton M, Jansson-Löfmark R, Äbelö A. Eflornithine elicits stereoselective extent of absorption: simultaneous population modeling of IV and oral pharmacokinetics in the rat and permeability in a modified Ussing chamber. (*Submitted*)

V. **Johansson CC**, Äbelö A, Jansson-Löfmark R, A retrospective time-to-event analysis of three eflornithine based treatments to evaluate effectiveness of oral eflornithine for treatment of late-stage *T.b. gambiense* infection. (*In manuscript*)

CONTENT

ABBREVIATIONS

BBB	Blood-brain barrier
BID	*Bis in diem*, *lat*. twice daily
bw	Bodyweight
CATT	Card agglutination test for trypanosomiasis
CI	Confidence interval
CL	Clearance
CL_D	Distribution clearance
cLogP	Calculated logarithmic octanol:water partitioning
CNS	Central nervous system
CSF	Cerebrospinal fluid
CV	Coefficient of variation
CYP	Cytochrome P450
DFMO	D,L-difluoromethylornithine
ID_{50}	Dose giving a 50% reduction in maximum response
F	Bioavailability
F_A	Fraction absorbed
FOCE	First-order conditional estimation
GOF	Goodness-of-fit
HAT	Human African trypanosomiasis
HBD	Hydrogen bond donor
HPLC	High performance liquid chromatography
IIV	Interindividual variability
IPRED	Individual prediction
KBR	Krebb's bicarbonate ringer solution
k_a	First-order absorption rate constant
k_{off}	Zero-order dissociation constant

k_{on}	First-order binding rate constant
k_{tr}	Transfer rate constant
LLOQ	Lower limit of quantitation
LogD	Logarithmic Octanol:water partitioning at pH 7.4
MS	Mass Spectrometry
MW	Molecular weight
NECT	Nifurtimox-eflornithine combination therapy
NMR	Nuclear magnetic resonance
ODC	Ornithine decarboxylase
OFV	Objective function value
P-gp	P-glycoprotein
PSA	Polar surface area
Q	Intercompartmental clearance
QC	Quality control
QID	*Quad in diem, lat.* four times daily
R_{max}	Maximum binding capacity
RSE	Relative standard error
T.b	*Trypanosoma brucei*
TID	*Tris in diem, lat.* three times daily
TMDD	Target mediated drug disposition
TTE	Time-to-event
UV	Ultraviolet
V	Volume of distribution
V_c	Central volume of distribution
V_p	Peripheral volume of distribution
VPC	Visual predictive check
WHO	World Health Organization

DEFINITIONS IN SHORT

Pharmacokinetics   What the body does to the drug [1].

Pharmacodynamics   What the drug does to the body [1].

1 INTRODUCTION

The present thesis focuses on the improvement of eflornithine treatment against late-stage African sleeping sickness. Current treatment alternatives are either liable to cause severe side effects, or difficult to manage due to logistical reasons, thus rendering a high cost of treatment. The present work has focused on elucidating stereoselective mechanisms and their implications when considering an oral treatment of the drug eflornithine, and methods to improve its oral absorption through development of a prodrug or new analog.

Eflornithine is a chiral molecule appearing with an L- and a D-enantiomer, currently being used for treatment of late-stage African sleeping sickness and is given as intravenous infusions for fourteen days. The stereoselective difference in pharmacokinetics and pharmacodynamics are important to quantify when considering an oral treatment.

The present thesis is based on five research papers, two (Papers I and II) dealing with the investigation of new treatment alternatives though an eflornithine prodrug or derivative and two papers (Papers III and IV) on the stereoselective pharmacokinetics of eflornithine *in vivo* in the rat. In the last paper (Paper V), a retrospective analysis, of public clinical data, comparing three different eflornithine-based treatment alternatives, oral eflornithine monotherapy, intravenous eflornithine monotherapy and a nifurtimox-eflornithine combination treatment, was performed by mathematical modelling

The chapters herein are organized accordingly, Chapter 1 offers a broad introduction to the disease area, current treatment alternatives and the theory behind the tools and methods that has been applied. Chapter 2 presents the specific thesis aims, Chapter 3-5 deals with the methods, results and discussions from each respective paper and Chapter 6 presents general conclusions in the thesis.

1.1 Human African trypanosomiasis

Human African trypanosomiasis (HAT) or human African sleeping sickness is caused by a parasite of the *Trypanosoma brucei* genus. There are two parasite subspecies infectious to humans', the *T.b. rhodesiense* and the *T.b. gambiense*. Both parasites are endemic to sub-Saharan Africa, and separated geographically by the Rift valley, stretching along the African continent [2].

The *T.b. rhodesiense* parasite is predominant in eastern and southern Africa. It causes an acute disease progression with initial clinical

manifestations such as a characteristic chancre and influenza-like symptoms occurring within a few weeks to months after infection [3, 4].

On the other hand the majority of reported cases (> 90%) are caused by the *T.b. gambiense* parasite, endemic to western and central Africa. *T.b. gambiense* causes a chronic form of infection with a slower onset [5]. The human host can be infected for years without signs of symptoms, however when symptoms do occur, the disease may already have progressed in to the late stage with central nervous system (CNS) involvement. The characteristic symptoms involve sleep disturbances, neurological disorders and alternations in mental state [6, 7, 8].

The parasite is transmitted by the tsetse fly (*lat. Glossina*) that can introduce the parasite to new hosts when it feeds on human or animal blood. When the fly ingests the parasite from an infected host, the parasite first must survive the fly's innate immune system. Surviving parasites migrate to the salivary gland were it is lodged until the fly feeds again and can then be transmitted to a new host [9]. The parasite's geographical spread is highly dependent on the fly, and only about 1% of the flies are infected by the parasite and there are several regions with tsetse flies that are not endemic to sleeping sickness [10]. Sleeping sickness is mostly present in remote and rural areas with limited access to healthcare and infrastructure [3].

The HAT disease progression is divided into two stages. In the early, haemolyphatic, stage the parasites have invaded the lymph nodes and systemic organs such as the liver and spleen [8]. If no treatment is received, the infection will progress into a late, encephalic stage, with parasites penetrating the blood-brain barrier (BBB) into the CNS. This late-stage is invariably fatal if no treatment is received [11, 17, 18].

Separating the two disease-stages is not easily done as symptoms may overlap. The early-stage is characterized by an array of diffuse symptoms including malaise, headache, fever and vomiting. These diffuse symptoms may cause confusion with malaria, and unnecessary antimalarial treatment is given instead [11]. Typical for the *T.b. gambiense* infection is also the Winterbottom's sign, which is the enlargement of the cervical lymph nodes [8]. In the late-stage, clinical symptoms involve psychiatric and mental disorders including sleep and motor disturbances. These sleep disturbances with a reversed sleep and wake cycle has given the disease its common name, sleeping sickness.

An early diagnosis is important for a better treatment outcome [4]. Diagnosis is preferably done serologically by laboratory examinations, since the clinical features are not specific enough [2]. For mass screening the card agglutination test for trypanosomiasis (CATT) can be used, however the positive predictive value of CATT is too low for it to be used as confirmatory diagnosis [4].

1.2 Drug treatment alternatives

For early-stage sleeping sickness there are better treatment alternatives available, including the drugs suramine and pentamidine. For late-stage, the treatment alternatives rely on old and unwieldy treatments with melarsoprol and eflornithine either as monotherapy or in combination with nifurtimox.

Suramine, used for early-stage *T.b. rhodesiense* is administered intravenously as a series of injections, five times daily every seventh day for 30 days. Due to hypersensitivity reactions that may occur, a test dose of 5 mg/kg is first administered followed by therapeutic doses of 20 mg/kg, with a maximum dose per injection of 1 g [2].

Pentamidine is recommended first-line treatment for early-stage *T.b. gambiense*. Due to its low bioavailability it is given as intramuscular injections or as intravenous infusions for 7 days with a daily dose of 4 mg/kg [4]. The most frequent side effects include pain at the injection site, hypoglycemia and hypotension. There are reports that suggest an emerging pentamidine resistance in some foci [19]. A possible oral prodrug approach to increase the oral bioavailability has been suggested for pentamidine [20].

Melarsoprol is an arsenic compound that has been used for treatment of late-stage sleeping sickness since the 1950's [21]. It is associated with very severe side effects such as encephalopathy leading to death in about 5% of treated patients [22, 23]. Melarsoprol is administered intravenously according to an injection scheme with varying doses and injection times [24]. An emerging resistance to melarsoprol has been reported [16, 25, 26].

1.3 Eflornithine

Eflornithine (DFMO; MW: 182.2 g/mol) is presented as a 50:50 racemic mixture of its L- and D-enantiomer. The pharmacologic effect is elicited through irreversible inhibition of the enzyme ornithine decarboxylase (ODC), an ezyme crucial for polyamine biosynthesis in all cells [27, 28]. The turn-over rate of the ODC enzyme has proven important for a successful treatment outcome. The ODC-turnover rate is slower in the *T.b. gambiense* parasite compared to both human and *T.b. rhodesiense* ODC, and thus they are less sensitive to eflornithine treatment [27, 29]. It has been argued that it is not the inhibition of the ODC with subsequent reduction of proliferative capacity that is causing the trypanostatic effect, but rather a reduction in the essential trypanothione antioxidant, that is responsible for the pharmacological effect [30]. The anti-proliferative activity of eflornithine requires an intact immune system to systemically eliminate the parasite [31, 32].
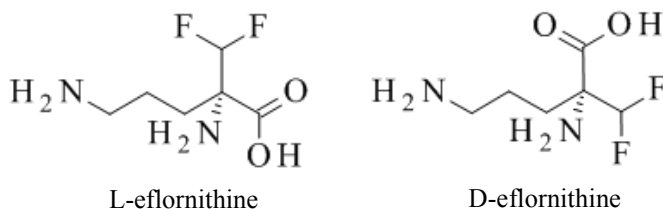
L-eflornithine   D-eflornithine

Figure 1. Molecular structure of eflornithine enantiomers.

Eflornithine was first developed as an intended anti-cancer treatment, though never marketed for that indication. The trypanostatic effects were discovered during the 1980's and eflornithine was registered for treatment of late-stage *T.b. gambiense* infection in 1990 [27]. Intravenous eflornithine monotherapy was up until recently the recommended first-line treatment against late-stage HAT [33, 34]. The introduction of a combination treatment consisting of intravenous eflornithine with oral nifurtimox has proven promoising in that fewer eflornithine doses for a shorter treatment period are required to achieve similar efficacy in HAT patients [35].

When used as monotherapy, eflornithine is administered as an intravenous infusion QID at a dose of 100 mg/kg for 14 days [11]. The recommended dose in children is higher, at 150 mg/kg, because of a lower CSF/plasma ratio that may result from a higher systemic clearance [36].

Eflornithine needs to be administered in a clinical-like setting with access to trained staff and sterile equipment [14]. The eflornithine treatment kit containing all necessary equipment and drug for one patient is also very bulky to distribute and store. All these aspects contribute to a high cost of treatment leaving many patients untreated [37].

An oral treatment is in high demand since it would facilitate the distribution of eflornithine and may reduce the overall cost, thus making treatment more readily available to patients in dire need. Previous attempts to develop an oral eflornithine treatment have failed, probably due to inadequate systemic drug exposure and that the high oral doses required are associated with dose limiting side effects [38].

1.4 Nifurtimox–eflornithine combination treatment

The introduction of the nifurtimox-eflornithine combination treatment has proved a relief to disease-ridden areas [35, 39]. In this combination, intravenous eflornithine (200 mg/kg BID for 7 days) is given along oral nifurtimox (15 mg/kg TID for 10 days). This has resulted in a reduction of

the total number of eflornithine infusions from 56 (in monotherapy) to only 14 when combined with nifurtimox. The mechanism of action for nifurtimox is argued, however generally believed to involve the formation of a free radical which is toxic to the parasites [40]. Thus, eflornithine and nifurtimox act on different targets and the pharmacological action may be described as independently joined as opposed to for example synergistic where the combined effect becomes multiplicative [41]. Nifurtimox monotherapy is used for treatment of Chargas disease, the Latin American variant of trypanosomiasis. But has on rare occasions been used as monotherapy in melarsoprol and eflornithine resistant HAT patients [42].

The recently introduced nifurtimox-eflornithine combination treatment has rendered a need for a further investigation into the possibility for an oral eflornithine dosage regimen.

1.5 Eflornithine PK and PD

Eflornithine is mainly (> 80%) renally cleared, no metabolites have been identified and the half-life in patients is about three hours [37, 43, 44]. No significant binding to plasma proteins has been observed [37, 43]. Successful eflornithine treatment depends on penetration through the BBB into the CNS. However, this penetration has been reported to be poor for eflornithine but with no stereoselective difference between the enantiomers [43]. Clearance and volume of distribution for eflornithine have previously been reported at 2 mL/min/kg and 0.35 L/kg, respectively in man [36]. Eflornithine has a oral bioavailability of 54% in man and about 50% in the rat, when analysed with nonstereoselective analysis [44, 45]. There are two prior publications discussing stereoselective bioavailability of eflornithine both in rat and man, with a reported enantioselective bioavailability of about 40 and 62% for L- and D-eflornithine, respectively in rat [45, 46].

The L- eflornithine enantiomer has previously been suggested to have a twenty-fold higher affinity to recombinant human ODC *in vitro* with K_D-values of 1.3 and 28.3 µM for L- and D-eflornithine, respectively [28]. The higher potency of L-eflornithine, compared to D-eflornithine, has been further confirmed in parasite cultures (Personal communication R. Brun Swiss Tropical Institute).

1.6 Gastrointestinal absorption

Oral administration is generally the preferred route for drugs as it is simple and enhances patient treatment adherence. The gastrointestinal tract is a

defense against hazardous substances entering the body and may be a difficult environment for the drug molecule, thus introducing hurdles to drug absorption. There are a number of barriers that a drug needs to penetrate in order to reach the systemic circulation. The fraction of the dose that reaches systemic circulation is referred to as the bioavailability (Figure 2) [47]. However, the generally accepted definition for bioavailability constitutes of both the extent of the dose that reaches systemic circulation and the rate at which the drug is absorbed [48, 49].

Drugs are often given in solid dosage forms and require disintegration and dissolution from the tablet form in order to be solubilized and absorbed. Only dissolved drug may permeate the gastrointestinal wall (Figure 2). Physiochemical properties of the drug molecule, such as size, hydrogen bonding or the partition coefficient will determine the route by which the drug penetrates the gut wall (Figure 3) [50, 51].

There are numerous different active carrier mediated transporters present in the gut wall and the compound's properties will determine its susceptibility for these active transporter proteins. The direction can be in two directions, influx and efflux, the best characterized efflux protein is P-glycoprotein (Pgp). A significant amount of metabolising enzymes such as CYP3A4 are present in the gut wall and may restrict the drug from reaching the systemic circulation [52, 53]. There are regional variations in the expression of these metabolising enzymes along the gastrointestinal tract [54, 55].
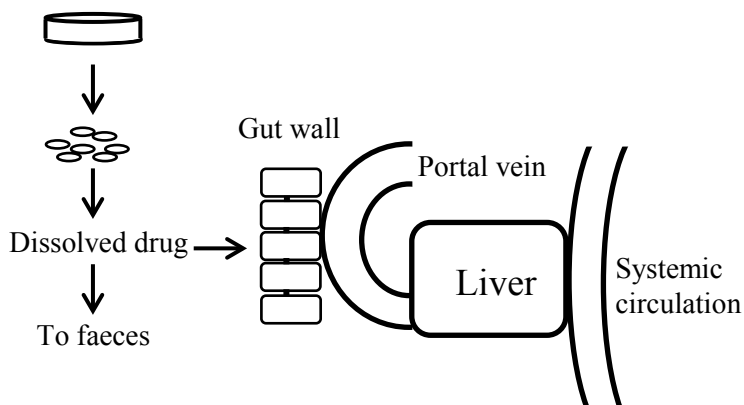

Figure 2. Schematic illustration on the general absorption process of drugs from solid dosage form to the systemic circulation. Figure is adapted from Rowland and Tozer [47].
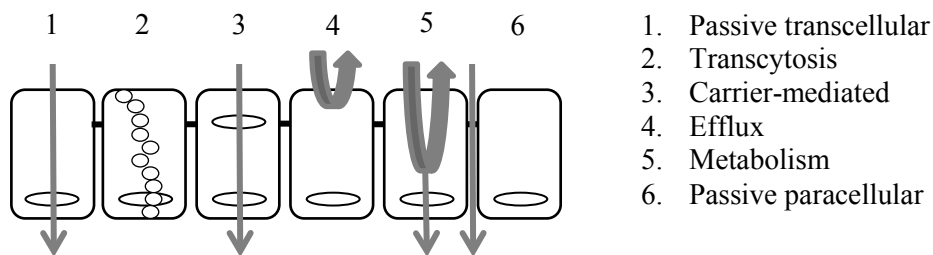
1. Passive transcellular
2. Transcytosis
3. Carrier-mediated
4. Efflux
5. Metabolism
6. Passive paracellular

Figure 3. Schematic illustration of gut wall absorption mechanisms. The figure is adapted from Stenberg *et al.* [56].

Endocytosis and trancytosis are the receptor-mediated routes of absorption for macromolecules [57]. The ligand binds to surface receptors on the enterocyte and is internalized in vesicles and absorbed. There are more than 400 membrane transport proteins that make up the carrier-mediated absorption mechanism [58]. Carrier-mediated transport can be either active, requiring ATP, or passive, relying on a concentration gradient. Active carrier-mediated transport maybe significant for large (> 250 g/mol) and hydrophilic compounds [51, 59]. In contrast to the passive processes, the active are expected to be saturable [58]. Carrier proteins are made up of chiral amino acids and have a rigid structure, thus the selectivity and specificity for these transport proteins is high and can be enantioselective.

The intercellular tight junctions are an intricate complex network of various proteins that normally pose a barrier for exogenous substances; however some drugs can also penetrate the junctional complex of the paracellular space [60–62]. Today, it is suggested to be included when screening new potential drug candidates [60].

1.7 Prodrugs

A prodrug is a pharmacologically inactive molecule that is metabolised both *in vitro* and *in vivo* into a pharmacologically active metabolite [63]. Common reasons for developing a prodrug can be to overcome poor aqueous solubility, high first pass extraction, chemical instability, and inadequate absorption over the gastrointestinal tract and BBB, pharmaceutical formulation difficulties, or toxicity. About 10% of all marketed drugs worldwide are prodrugs and the number is increasing [64–66].

The most common prodrug is an ester derivative which is developed to enhance the lipophilicity of the compound and thus the passive membrane

permeability. Esters are readily hydrolyzed by ubiquitous esterases, common throughout blood, liver and other organs and tissues [65, 66]. Amide prodrugs are more stable and often developed in order to improve gastrointestinal absorption after oral administration. They are less common than esters because of higher metabolic stability *in vivo* [65]. Metabolism of amides depends on hydrolysis by carboxylesterases, peptidases and proteases.

1.8 Mixed effects modelling

Mixed effects modelling enables the simultaneous incorporation of all available data across different treatments, doses, studies and populations. Not only can the mean values (typical values) be estimated in the population but also the random effects such as within and between subject and/or study variability [67]. This approach makes it possible to utilise imbalanced or very sparse observational data to investigate also complex models. This is not easily done using the standard approach where each study subject is modelled separately and then pooled.

Mixed effects modelling enables separating out the fixed effects and the random effects. Fixed effects describe the underlying system such as the pharmacokinetics of a drug, through the population primary pharmacokinetic parameters, in this case: volume of distribution and clearance. In the most simplified form described using the one-compartment model after intravenous administration (Eqaution 1) for the plasma concentration-time profile.

$$C_p = \frac{Dose_{iv}}{V} \cdot e^{\left(-\frac{CL}{V}t\right)} \tag{Eq. 1}$$

where C_p is the plasma concentration predicted for the typical patient based on the given dose, the volume of distribution (V) and the elimination clearance (CL) over time (t).

The mixed effects modelling approach enables a separation between the variability that can be observed between study subjects and occasions (inter-individual variability, IIV; inter-occasion variability, IOV) and the variability that can occur due to study-specific errors, such as bioanalysis, sampling and dosing. The between subject variability can be described by equation 2:

$$P_i = P_{pop} \cdot e^{\eta_i} \tag{Eq. 2}$$

where P_i is the individual parameter estimate, P_{pop} is the typical value for that specific parameter in the population and η_i is describing the difference between the population mean and the individual prediction of the parameter. Normal distribution of η is assumed with mean zero and variance ω^2. The

individual parameter estimates (P_i) are assumed to be log-normal distributed (Equation 2).

The between subject variability can be described using different patient specific characteristics also known as covariates. Covariates can be either continuous measurements such as bodyweight and creatinine clearance or categorical *e.g.* gender. The covariate is included to explain the population variability of that specific parameter. The relationship between the covariate and the parameter can be described using different functions, for example: linear, exponential, power or proportional. The covariate relationship to the individual parameter using a linear approach can be described by:

$$P_i = P_{pop} + \theta \cdot BW \qquad \text{(Eq. 3)}$$

where P_i is the individual parameter estimate, P_{pop} is the typical value for that specific parameter in the population, θ is the slope of the linear relationship between the parameter and bodyweight (BW) in this example. The incorporation of covariates into the model aims to reduce the unexplained variability, η. Variability that cannot be described by any other approach is modelled using a residual error model, such as:

$$Y_i = IPRED + \varepsilon_i \qquad \text{(Eq. 4)}$$

where Y_i is the individual observation, *IPRED* is the individual prediction and ε is the residual error with a mean zero and variance σ^2. Equation 4 describes the additive residual error model however other residual error models can also be used such as proportional or a combination of proportional and additive.

1.9 Target mediated drug disposition

A drug with a relatively high affinity to an abundant target receptor may display target mediated drug disposition (TMDD) [68]. These two factors must interplay to a high enough extent to impact the pharmacokinetics of the drug through an exposure dependent effect in volume of distribution and clearance [69]. This type of nonlinear pharmacokinetics has been observed for angiotensin converting enzyme (ACE) inhibitors, the drug paclitaxel and many of the antibody-based drugs currently investigated [69, 70]. The general TMDD model proposed by Mager *et al.* consisted of three compartments where unbound drug can distribute to a binding compartment and be associated with the target to form a drug-receptor complex (DR) (Figure 4) [69].
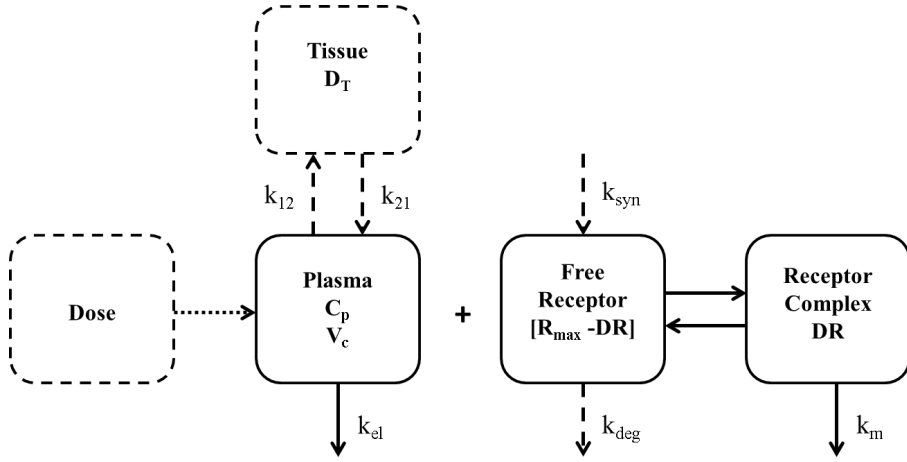
Figure 4. The general model for drugs displaying target mediated drug disposition, adapted from Mager *et al.* with model equations defined below (Equations 5 to 8) [69]. C_p is the drug plasma concentration, V_c is the central volume of distribution, DT is drug in tissue, k_{el} is the elimination rate constant from the central compartment, k_{12} and k_{21} are the distribution rate constants to the peripheral compartment. R_{max} is the total receptor amount, DR is the drug-receptor complex, k_{syn} and k_{deg} are the rates of synthesis and degradation of the complex and k_m is the elimination rate constant of the complex.

The TMDD model is described by the following differential equations:

$$\frac{dC}{dt} = In(t) - (k_{el} + k_{12}) \times C_p + k_{12} \times \frac{D_T}{V_c} - k_{on} \qquad \text{(Eq. 5)}$$

$$\times (R_{max} - DR) \times C_p + k_{off} \times DR$$

$$\frac{dD_T}{dt} = k_{21} \times C_p \times V_c - k_{12} \times D_T \qquad \text{(Eq. 6)}$$

$$\frac{dDR}{dt} = k_{on} \times (R_{max} - DR) \times C_p - \left(k_{off} + k_m\right) \times DR \qquad \text{(Eq. 7)}$$

$$\frac{dR_{max}}{dt} = k_{syn} - k_m \times DR - k_{deg} \times (R_{max} - DR) \qquad \text{(Eq. 8)}$$

where *In(t)* in equation 5 describes the input of drug into the system.

However, determining if a drug exhibits TMDD cannot be based on the pharmacokinetics alone, additional information and experiments are required and one often depends on the direct quantities of the drug in relevant tissues for supporting information [68].

1.10 Time-to-event analysis

To elucidate the efficacy of a treatment in a clinical trial, one may assess the time to reach a predetermined event, such as relapse, treatment failure or death. An example of such an analysis was described by Cox *et al.*, where the anti-emetic effect of ondansetron was investigated [71]. Comparing within and between studies can be challenging since the follow-up time period may be different. The exact time of an event may not be known, but only that it occurred within a time interval. This can be handled through interval censoring. If no event has occurred at the end of follow-up the individual is regarded as a survivor and data is right censored. The possibility to incorporate censoring differentiates the time-to-event analysis from classic statistical approaches [72].

The Kaplan-Meier approach is a nonparametric way of describing the time to an event and does not allow for simulations. In a parametric approach to the time to event analysis a distribution of the hazard is assumed and the underlying system parameters are estimated. The distribution can have different shapes, such as exponential, Weibull or Gompertz. In its simplest form the exponential distribution assumes a constant hazard over time, whilst the Weibull can assume different shapes through estimation of the shape parameter. The different shapes of the Weibull function makes it useful since it can describe both increasing and decreasing hazard with time as well as an exponential, time constant hazard distribution. The event free survival is estimated by the survival function *S(t)*:

$$S(t) = \Pr(T > t) = \exp\left(-Ln2\left(\frac{t}{\varphi}\right)^{\gamma}\right) \qquad \text{(Eq. 9)}$$

And the probability density function *p(t)*:

$$p(t) = \Pr(t = t) = Ln2 \times \frac{\gamma}{t} \times \left(\frac{t}{\varphi}\right)^{\gamma} \times \exp\left(-Ln2 \times \left(\frac{t}{\varphi}\right)^{\gamma}\right) \qquad \text{(Eq. 10)}$$

where the two parameters, hazard (φ) and shape (γ) can be estimated.

The hazard for an event is related to the time-to-event using the following relationship (Equation 11).

$$\lambda = \frac{1}{mTTE} \times \left(-\log(0.5)^{\frac{1}{\gamma}}\right) \qquad \text{(Eq. 11)}$$

where (λ) is the hazard, mTTE is the median time to event and γ is the Weibull shape parameter.

2 AIM

The overall aim of this thesis was to improve the treatment against late-stage human African trypanosomiasis through investigating possible alternative approaches to an oral eflornithine treatment. To better understand why an oral dosage regimen so far has failed and how the treatment may be improved, the following specific aims were addressed:

1. To investigate possible prodrug candidates with regards to *in vivo* exposure of eflornithine and *in vitro* anti-trypanosomal activity. (Paper I)

2. To assess and investigate the deficient *in vivo* exposure of eflornithine after oral administration of prodrug candidates, with regards to *in vivo* eflornithine exposure and *in vitro* permeability and metabolic stability. (Paper II)

3. To develop a model for the intravenous stereoselective pharmacokinetics of eflornithine in the rat and investigate *in vivo* absorption by means of deconvolution. (Paper III)

4. To investigate and model possible oral absorption mechanisms of L- and D-eflornithine separately, and assess proposed model in Paper III when simultaneously modelling IV and PO eflornithine pharmacokinetic data. (Paper IV)

5. To compare treatment outcome of three different eflornithine based treatments in man, based on published clinical data and to investigate possible positive effects of a combination treatment. (Paper V)

3 PATIENTS AND METHODS

3.1 Paper I – Synthesis of eflornithine derivatives

3.1.1 General procedure for synthesis eflornithine derivatives

The prodrug candidates (CD) were synthesized, here exemplified by candidate CD1 (Figure 5) where ethanol was coupled to the carboxylic acid on eflornithine under constant reflux and the presence of thionyl chloride. The synthesis was based on a previously described method [73].
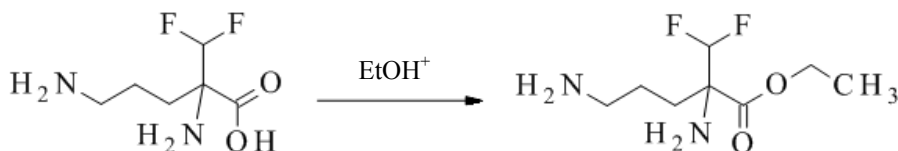

Figure 5. Reaction scheme for the prodrug candidate CD1, an ethyl ester.

The product was evaporated to dryness and the ethyl ester was purified by column chromatography. The α- and δ-amines were also used for attaching substituents for other proposed prodrug candidates, molecular structures are shown in scheme 2 to 4, Paper I. The structures were confirmed using NMR and MS.

3.1.2 *In vivo* investigation of prodrug candidates

A general method for animal surgery and blood sampling used throughout the studies included in the thesis (Papers I, II, III, IV) is described below.

Male Sprague-Dawley rats were purchased from Charles River, Germany, weighing about 300 g. The animals were housed at a certified animal facility, Experimental Biomedicine at Gothenburg University, Sweden. Animals were left to acclimatize for at least 5 days after arrival. The rats were housed in 12 h light-dark cycles, at 25-27°C and at 60-65% humidity. Rats were kept four-by-four until surgery and thereafter separately to prevent damage to sutures and catheters during recovery. Food (Harlan, USA) and tap water were available before and after surgery *ad libitum*, the feed was removed 8 h prior to drug administration whereas water was available at all times. All surgical experiments were performed during the

light phase of the cycle, however blood sampling was done during both. All animal experiments were in accordance with approved ethics applications 255/2005, 313/2008 and 352/2008 to the Ethics Committee for Animal Experiments, Gothenburg, Sweden.

Eflornithine hydrochloride monohydrate (MW 236.65 g/mol) was kindly donated by WHO/TDR (Geneva, Switzerland). Isoflurane (Forene; Abbot Scandinavia AB, Solna, Sweden) and heparin (Leo Pharma AB, Malmö, Sweden) were purchased from Apoteket AB (Sweden).

Rats were anesthetized by inhalation of isoflurane (2.9-3.7%) in air. The left jugular vein was catheterised using a MRE040 tube (1.02 mm × 0.64 mm) purchased from AgnThos (Lidingö, Sweden) prefilled with 100 IU/ml heparin in saline solution. The catheter was tunnelled subcutaneously and emerged though skin in the back of the neck. All animals were allowed to recover overnight after surgery before engaged in any further experiments.

Eflornithine or prodrug candidates were dissolved in saline solution (0.9% NaCl in MilliQ-water) to reach the target concentration that would generate an oral dose equivalent in molar amounts to an eflornithine dose of 100 mg/kg in the rat. Two compounds, CD3 and CD6 were first dissolved in DMSO before further diluted with saline to reach the target concentration.

The oral solution containing either eflornithine or prodrug candidate was administered via gavage (5 ml/kg) to the rat. Blood samples were drawn from the catheter in the right jugular vein. The catheter was flushed with heparinised saline solution (20 IU/ml) after each sampling occasion to prevent blood clotting. Blood sample volumes were replaced in the rat with an equal volume of saline solution. Eight blood samples of 250 µL per sample were taken from each rat at predetermined times for up to eight hours after drug administration. The blood samples were directly transferred to heparin pre-treated tubes and centrifuged at $12000 \times g$ for 8 min to separate the plasma. The plasma supernatant was transferred to sodium fluoride (NaF) and EDTA pre-treated tubes (Teklab Scariston, Durham, UK), vigorously shaken and stored at -80°C until further analysis.

For quantitation, the plasma samples were thawed and a 75 µL aliquot was mixed with ice cold methanol for protein precipitation. The samples were vigorously-shaken for 15 s and refrigerated at 4°C for about 30 min and then shaken again. To separate the protein precipitate, samples were centrifuged at $12000 \times g$ for 10 min and then frozen at -20°C for 10 min to freeze the pellet. The supernatants were decanted into new tubes and evaporated to dryness at room temperature under a gentle stream of air for 2-3 h. The dried samples were re-dissolved in 100 µL deionized water, shaken for 15 s and centrifuged for 5 s. The samples were transferred to injection vials which were loaded into the autoinjector for analysis.

D- and -L-eflornithine were quantitated in plasma after an oral dose of

prodrug candidate using an enantioselective HPLC bioanalysis method [46].
The analytical procedure is described in detail in chapter 3.3.3.

3.1.3 *In vitro* anti-trypanosomal activity screen

The *in vitro* anti-trypanosomal activity of the prodrug candidates was
assessed in incubations with *Trypanosoma brucei brucei* parasites.

The drug sensitivity assay was based on a previously described method by
Vodnala *et al*. [15]. The bloodstream variant of the *T.b. brucei* parasite was
seeded on a 96 well cell culture plate and incubated at $37^{o}C$ in Dulbecco's
modified eagle medium (D-MEM), containing 10% heat inactivated calf
serum, 20 mM HEPES, 0.14% glucose, 1.5% $NaHCO_3$, 2 mM L-glutamate,
0.14 mg/mL gentamycin, 0.3 mM dithiothreitol (DTT), 1.4 mM sopdium
pyruvate, 0.7 mM L-cysteine, 28 µM adenosine and 14 µM guanosine. At
least 8000 parasites per well was confirmed by manual counting under
microscope.

Incubations were performed in triplicates at concentrations of 0.16, 0.8,
4 and 20 µM of eflornithine or prodrug candidate in a total volume 100 µL
per well. After 72 hours of incubation, 10 µL of WST-1 cell proliferation
reagent (Roche Diagnostics, Mannheim, Germany) was added to each well
and the plate re-incubated for 2 hours at $37^{o}C$. The WST-1 reagent enables
monitoring of the conversion from tetrazonium salt (WST-1) to formazan by
living cells, in this case *T.b. brucei* parasite. Parasite viability in the
incubations was then assessed using multiwell scanning spectrophotometer
with an excitation wavelength of 450 nm. The difference in dye absorbance
between WST-1 (light red) and formazan (dark red) enables a quantification
of the cell viability in each well and consequently sensitivity to eflornithine
or the prodrug candidates. Separate IC_{50}-values was estimated using
WinNonLin version 6.2 (Pharsight Co., St. Louis, MO, USA) for each
investigated prodrug candidate.

3.2 Paper II –Deficient eflornithine exposure *in vivo* after oral dose of prodrug candidate

3.2.1 *In silico* predictions of physicochemical properties

The molecular structure of each prodrug candidate is shown in figures 1 and
2 in Paper II. General physicochemical properties for each of the prodrug
candidates were predicted using an online prediction tool, Molinspiration

(http://www.molinspiration.com/cgi-bin/properties). The number of hydrogen bond donors (HBD) and the polar surface area (PSA) were used for prediction of fraction absorbed as implemented in SimCYP version 7.10 (SimCYP Ltd, Sheffield, UK).

3.2.2 Experimental *in vivo* design

Each of the prodrug candidates or racemic eflornithine hydrochloride was separately administered to the rat via oral gavage. Oral doses of prodrug candidate corresponded to an equimolar eflornithine dose of 100 mg/kg. Blood samples were taken 30 minutes prior to administration of any compound and at predetermind times 30, 60, 105, 150, 210, 270, 360, 480 and 1140 minutes after dose. A total of 10 samples of 200 μL blood were taken from each rat and replaced with an equal volume of saline solution. Plasma samples were stored at -80°C until quantitation of L- and D-eflornithine using the method described in chapter 3.3.3.

3.2.3 Animal surgery and rat liver microsome preparation

Two rats were decapitated and the livers were excised. The separate livers were minced and mixed with sucrose solution (0.25 M sucrose, 10 mM TRIS, 1 mM EDTA, pH 7.4). The mixture was in several steps centrifuged and homogenized to separate the liver microsomes. First, the homogenate was centrifuged at 20000 × g (Sorvall Super T 21 centrifuges, Newtown, Connecticut, USA) for 20 minutes at 4°C. Second, the supernatant was transferred to new tubes, re-suspended, homogenized and further centrifuged in two steps at 100 000 × g for 60 minutes each. The final microsomal pellet was again homogenized and resuspended in TRIS-buffer (0.1 M TRIS, 20% glycerol, 0.1 mM EDTA, 0.1 mM DTT, pH 7.4) and frozen at -80°C until further usage.

3.2.4 *In vitro* microsomal incubation conditions

A bicinchoninic acid (BCA) assay was used to assess the protein quantity in pools of rat liver microsomes [74]. Bovine serum albumin was used for the standard curve, correlating the protein concentration to UV-absorbance, measured by a Helios γ spectrometer (Unicam UV-Visible spectrometry, Cambridge, Great Britain). The standard curve concentrations ranged from 25 to 1000 μg/mL and absorbance was measured at 562 nm.

Racemic eflornithine and the prodrug candidates were incubated separately at concentrations of 10, 100 and 1000 µM with the rat liver microsomes in a phosphate saline buffer (10 mM, pH 7.4). Samples (60 µL) were taken from the incubation phosphate buffer at fixed time points 0, 30, 60 and 90 minutes of incubation. The incubation reaction was stopped by adding 60 µL of ice-cold methanol. The samples were vigorously-shaken for 10 s, centrifuged at $12000 \times g$ for 10 minutes and the supernatant transferred to a new tube and stored at -80°C until further analysis.

All incubations were performed under aerobic conditions at 37°C and at a protein concentration of 0.5 mg/mL in buffer. The pore forming agent alamethicin, a NADPH regenerating system (1.3 mM NADP, 3.3 mM G6P, 0.4 U/mL G6PD and 5 mM $MgCl_2$) and DMSO (1% v/v in final mixture) were added to the incubation phosphate saline buffer prior to incubation.

Along the prodrug candidates, positive controls for enzymatic activity: chloramphenicol succinate (CAPS) and procainamide (PA) were incubated with the rat liver microsomes. CAPS and PA were incubated at 1000 and 100 µM respectively, and all incubations were performed in triplicates. Both the formation of metabolite and depletion of CAPS and PA were quantitated.

3.2.5 *In vitro* permeability, Caco-2 cell assay

The general method for the Caco-2 cell assays and sample handling was used throughout Papers II and III, the assay was based on a previously described method by Hubatsch *et al*. [75].

Caco-2 cells with a high passage numbers (95 to 97 passages) were grown for 23 to 25 days, seeded onto permeable polycarbonate filters with a pore size of 0.4 µm and a diameter of 12 mm on a 12-well cell culture plate (Corning Costar, Lowell MA USA) in cell culture media (DMEM). A preincubation 24 hours prior to the permeability assay was initiated by transferring the filters with seeded Caco-2 cells to fresh DMEM. After preincubation, the filters were carefully decanted from DMEM and transferred to preheated (37°C) Hank's balanced salt solution (HBSS, pH 7.4) buffer and again incubated at 37°C for 20 minutes under gentile agitation and aerobic conditions.

The transepithelial electrical resistance (TEER) was recorded before and after the permeability assay using chopstick electrodes and Evohm epithelial voltmeter (WPI, Sarasota FL USA). Paracellular permeability was assessed between batches of Caco-2 cells using radiolabelled ^{14}C-mannitol (Perkin Elmer Waltham MA USA, 50 Ci/mol, 0.1 mCi/mL, 5 µL/mL in HBSS stock solution) as reference.

Racemic eflornithine and the prodrug candidates were dissolved in DMSO, mixed with ^{14}C-mannitol and diluted to a final concentration of 10 mM with HBSS buffer. The apparent permeability (P_{app}) over Caco-2 cell monolayers was investigated in both apical-to-basolateral (ab) and basolateral-to-apical (ba) direction. Samples were taken from both the donor and receiver side of the monolayers at fixed times, up to 90 minutes after addition of drug substance. Sample times from the receiver compartment were: 15, 30, 60 and 90 minutes and from the donor compartment: 0 and 90 minutes. An equivalent volume of pre-tempered HBSS was replaced in the respective donor or receiver compartment.

3.2.6 Chiral eflornithine quantitation

L- and D-eflornithine was quantitated separately in rat plasma and in HBSS buffer using the stereoselective bioanalysis method described in chapter 3.3.3.

The separate enantiomers were quantitated in rat plasma after oral administration of either racemic eflornithine or the investigated prodrug candidates. The standard curve and quality control (QC) samples were prepared in human plasma at concentrations ranging from 3 to 2500 µM and from 10 to 1250 µM, respectively.

For eflornithine quantitation in HBSS after incubation with rat liver microsomes, a florescence detector (Jasco 821-FP Spectroflurometer, Jasco, Tokyo, Japan) was used for increased sensitivity and a lower limit of detection. Eflornithine standards and QC samples were prepared in phosphate buffer and concentrations ranged from 0.05 to 50 µM and 2.5 to 40 µM, respectively.

3.2.7 Quantitation in phosphate buffer, microsomal incubations

The positive control in the microsomal incubations, procainamide (PA), was quantitated simultaneously with the formed metabolite, para-aminobenzoic acid (PABA), in HBSS buffer based on a previously reported HPLC method [76]. The present HPLC-system consisted of an Agilent 1260 Inifinity binary pump, an Agilent 1260 Inifinity standard autosampler, an Agilent 1260 Infinity Thermostated Column compartment (Agilent Technologies, Santa Clara CA , USA), and a Shimadzu SPD 10-A UV-vis detector (Shimadzu Corp., Kyoto, Japan). Data was acquired using Clarity Chromatographic version 3.0.3 (Dataapex, Prague, Czech Republic). Separation was achieved on a Kinetex C_{18} column (Kinetex 2.6 µm 100 × 4.6 mm, Phenomenex,

Torrance, CA, USA) at 40°C. A gradient flow was used, at a flow rate of 0.4 mL/min and the gradient from 100% phosphate buffer (25 mM, pH 2.6) changed linearly to 15% acetonitrile, 25% methanol and 60% phosphate buffer over 3 minutes, maintained for 10 minutes and returned to 100% phosphate buffer (25 mM, pH 2.6) then re-equilibrated for 10 minutes. A calibration curve and QC samples were prepared in HBSS buffer, the concentrations ranged from 2 to 8000 µM and 25 to 3000 µM, PA and PABA respectively. The mean retention time was 6.1 minutes for PA and 7.4 minutes for PABA.

The quantitation of chloramphenicol succinate (CAPS) and the metabolite chloramphenicol (CAP) in HBSS buffer after incubation with rat liver microsomes was based on a previously developed method [77]. The HPLC system consisted of a Shimadzu LC-10AD pump (Shimadzu Corp., Kyoto, Japan), an 87-well MIDAS 830 auto-injector (SparkHolland, Emmen, The Netherlands) and a Shimadzu SPD-10A UV-VIS detector (Shimadzu Corp., Kyoto, Japan). CAP and CAPS were separated on a C_{18}-column (Chromolith Performance, RP-18e, Merck KGaA, Darmstadt, Germany), with the flow rate 2 mL/min of mobile phase consisting of acetate buffer (0.5 M, pH 5.5) with 40% methanol and the counter ion, TBA at a concentration of 0.625 mM. A calibration curve and QC samples were prepared in HBSS buffer and concentrations ranged from 2 to 8000 µM and 25 to 3000 µM for CAPS and CAP, respectively. The mean retention times were 1.7 and 1.9 minutes for CAP and CAPS, respectively.

3.2.8 Quantitation in HBSS buffer, Caco-2 experiments

Quantitation of both the prodrug candidates and eflornithine (non-stereoselective) in HBSS buffer was achievable by liquid chromatography and mass spectrometry.

The LC-MS/MS system consisted of a Thermo Quantum Discovery triple-quadrupole mass spectrometer coupled to a Waters Aquity UPLC system in positive ion mode. Due to the different polarity of the compounds, two separate methods were set up. In the first method, method 1, separation required a gradient flow of two mobile phases.

Phase A, consisted of aqueous 0.1% formic acid with 5% acetonitrile and Phase B of 0.1% formic acid in acetonitrile. The gradient flow was from 1 to 90% of mobile phase B over two minutes, and separation was achieved over an Aquity UPLC HSS T3, 1.8 µm 2.1×50 mm column. In Method 2, the gradient flow was from 99 to 50% of mobile phase B over two minutes and separation was achieved on an Aquity UPLC BEH Amide 1.7 µm 2.1×50

mm column. The LC-MS settings for each of the investigated compounds are summarized in Table 1, Paper II.

3.2.9 Data analysis

The apparent permeability over Caco-2 cell monolayers was calculated using equation 12 and assuming sink conditions.

$$P_{app} = \frac{dQ}{dt} \times \frac{1}{A \times C_0} \qquad \text{(Eq. 12)}$$

where P_{app} is the apparent permeability (cm/s), dQ/dt is the net flux of compound at a given time (mol/s), A is the exposed filter area (cm^2) and C_0 is total concentration (mol/L) in the donor compartment at the beginning of the experiment. A Hill type correlation between Caco-2 P_{app} and fraction absorbed after oral administration to man of 21 compounds, reported by Stenberg *et al*., was used for predicting the oral fraction absorbed for the compounds investigated herein based on the observed Caco-2 P_{app} [78, 79].

After microsomal incubation, the simultaneous first-order rate for depletion of CAPS and formation of CAP was estimated using WinNonLin version 6.2 (Pharsight Co., St. Louis, MO, USA). The biotransformation of PA and PABA was quantitated similarly.

3.3 Paper III – Stereoselective pharmacokinetics of eflornithine

3.3.1 Experimental *in vivo* design

Racemic mixture of eflornithine was administered as an intravenous infusion or as an oral single dose to the rat. The study design is summarized in the table below (Table 1). Eflornithine was dissolved in saline solution and pH was adjusted to 7.2 with sodium hydroxide prior to intravenous infusion. The infusion rate profiles were designed to result in plasma concentration-time profiles mimicking those obtained after oral administration of different doses. Intravenous infusion volumes were 5 mL/kg, the rat was moving freely and the catheter was connected to a balance arm and swivel during the infusion. The total volume of the oral gavage was 10 mL/kg. Arterial blood samples, 7 up to 13 of 150 µL each were collected from each rat for quantitation of eflornithine enantiomers. Faeces were collected from rats receiving eflornithine orally to assess the fraction between the eflornithine enantiomers remaining in the intestine.

Table 1. Experimental design for the *in vivo* study in the rat.

Route of administration	Racemic dose (mg/kg of bw)	Length of infusion (min)	No of rats
Intravenous	100	60[a]	5
	550	160 - 163	5
	2700	400	5
Oral	40	-	5
	150	-	5
	400	-	6
	1200	-	5
	3000	-	5

[a] one rat at this dose level received half the racemic dose during a 60 minute infusion and the remaining amount as a 10 minute infusion.

3.3.2 Caco–2 cell permeability

Bidirectional apparent permeability of the eflornithine enantiomers was investigated over Caco-2 cells. The method and assay set-up was similar to the previously described in chapter 3.2.5.

Racemic eflornithine donor concentrations of 0.75 and 12.5 mM were investigated and samples were taken at regular time intervals 0, 40, 80, 120 minutes after addition of drug. The apparent permeability was assessed in both apical-to-basolateral and basolateral-to-apical direction and in the presence of a Pgp-inhibitor (GF120918, 0,01 mM). Eflornithine was incubated with only the polycarbate filter, without the Caco-2 cells, to study the possibility of the filters being a barrier for eflornithine.

The apparent permeability for the separate enantiomers was derived using equation 12.

3.3.3 L – and D – eflornithine determinations in plasma

A previously published bioanalysis method was applied for enantioselective determinations of L- and D-eflornithine in rat plasma samples [46]. Since eflornithine does not have a chromophore, UV detection was possible only after pre-column derivatization with o-phtalaldehyde (OPA). Chiral separation of the enantiomers was possible by derivatization with N-acetyl-L-cysteine to form the diastereomeres.

The HPLC system constituted of two Shimadzu LC-10AD pumps (Shimadzu Corp., Kyoto, Japan), a 48-well Endurance Prospect 2 auto-injector (SparkHolland, Emmen, The Netherlands) and a Shimadzu SPD-10A

UV-VIS detector at 340 nm wavelength (Shimadzu Corp., Kyoto, Japan). L- and D-eflornithine was separated over two serially connected C_{18}-columns (Chromolith Performance, RP-18e, Merck KGaA, Darmstadt, Germany). Data acquisition was done by Chromatographic station for Windows (CSW) version 1.2.3 (Dataapex, Prague, The Czech Republic). Separation was dependent on a gradient flow of two separate mobile phases.

Mobile phase A consisted of: tris(hydroxymethyl)aminomethane buffer (0.1M, pH 6.8) at 82% and 18% methanol. Mobile phase B contained 70% methanol in MilliQ-water, the flow rate was 2 mL/min and the gradient was: t = 0-16 min 100% mobile phase A, t = 16-17 min a linear decrease of mobile phase A from 100 to 0% and t = 17-20 min a linear increase of mobile phase A from 0 to 100%.

A comparison of standards prepared in human and rat plasma was performed to ensure that human plasma would be a clean matrix for preparation of the eflornithine calibration curve and QC samples for quantitation in rat plasma samples. The two matrices showed good homology and the calibration curve was prepared in human plasma with racemic eflornithine concentration ranging from 3 to 2500 µM. The QC samples ranged from 3 to 1000 µM and were analysed in triplicates within every run. The accuracy and precision of each analytical assay were within 15%.

3.3.4 Eflornithine quantitation, Caco–2 cells

L- and D-eflornithine were quantitated in HBSS buffer samples from the Caco-2 cell assay. The sensitivity of the method was increased using a fluorescence detector, Jasco 821-FP Intelligent Spectrofluorometer (Jasco, Tokyo, Japan) at a wavelength of 340/440 nm (excitation/emission).

A calibration curve ranging from 0.0127 to 750 µM was prepared in HBSS buffer, the lower range (0.0127 to 1.03 µM) was determined using the fluorescence detector, and the upper range (3.09 to 750 µM) using the UV detector. The HBSS samples did not require samples work-up and were injected directly onto the HPLC. Samples at the highest incubation concentration (750 µM) were diluted to fall within the calibration curve range.

3.3.5 Eflornithine quantitation in rat faeces

L- and D-eflornithine were quantitated in faeces after oral administration of racemic mixture to the rat using the aforementioned method, in chapter 3.3.3

A reference curve was prepared using faeces from drug free rats, by mixing the faeces dissolved in Milli-Q water with stock solutions of eflornithine. The reference curve ranged from 5 to 3000 µM of eflornithine

and blank samples were used to ensure that there was no interference from
endogenous substances in the faeces.

Faeces were collected from rats receiving oral eflornithine and
droppings were dissolved in Milli-Q water (4 droppings in 2 mL of water).
The solution was incubated at room temperature for 30 minutes under gentile
agitation, then mixed with ice-cold methanol and refrigerated for another 30
minutes. The samples were centrifuged in two steps, first at 1770 × g for 6
minutes; the supernatant was then transferred to a new tube and centrifuged
again at 12000 × g for 10 minutes. The supernatant was transferred to a new
tube and evaporated until dryness under a gentle stream of air at 50°C. The
samples were re-dissolved in Milli-Q water and a 75 µL sample was
transferred to injection vials which were placed in the HPLC auto-injector.
Samples outside the highest reference concentration were diluted.

3.3.6 Pharmacokinetic data analysis

The L-and D-eflornithine plasma concentration-time profiles after
intravenous infusion to the rat were analysed by a population approach using
the software NONMEM version 7.12 (Icon Development Solutions, Ellicott
City, Maryland, USA) [80]. Model files and graphics were handled using
Piraña version 2.6.1 and the R based programs Xpose4 and PsN version 3.5.3
[81–83].

The proposed three-compartment model with nonlinear binding to one of
the peripheral compartments (Figure 6), was a modification of two previously
described models, one general model describing target mediated drug
disposition (TMDD) and one model describing the saturable peripheral
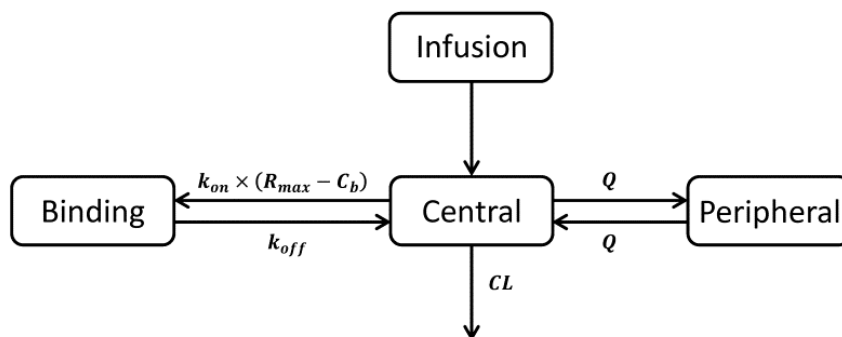distribution of paclitaxel [70, 69].

Figure 6. The proposed pharmacokinetic model describing the plasma concentration-
time profiles of eflornithine after intravenous administration to the rat. Abbreviations
are described in detail below in the corresponding model equations.

The rate of change in drug concentration in the central compartment (C_p) was defined as:

$$\frac{dC_p}{dt} = \frac{In(t)}{V_c} - \left(\frac{CL}{V_c} + \frac{Q}{V_c}\right) \times C_p + \frac{Q}{V_t} \times C_t - k_{on} \times C_p \qquad \text{(Eq. 13)}$$

$$\times (R_{max} - C_b) + k_{off} \times C_b$$

where *In(t)* is the infusion of drug into the central compartment. V_c and V_t are the volumes of distribution in the central and peripheral compartments respectively. C_t is the concentration in the peripheral compartment. CL is the clearance from the central compartment; Q is the intercompartmental clearance and k_{on} the binding rate constant, k_{off} the dissociation rate constant and R_{max} the total binding capacity of the target. The rates of change in drug concentrations of the first and second peripheral compartments were defined by the following equations (Equation 14 and 15).

$$\frac{dC_t}{dt} = \frac{Q}{V_c} \times C_p - \frac{Q}{V_t} \times C_t \qquad \text{(Eq. 14)}$$

$$\frac{dC_b}{dt} = k_{on} \times C_p \times (R_{max} - C_b) - k_{off} \times C_b \qquad \text{(Eq. 15)}$$

where C_b is the drug concentration in the second peripheral binding compartment.

L- and D-eflornithine intravenous population pharmacokinetic parameters were used to generate individual plasma systemic input rate functions from the gut using a deconvolution method of oral data. Ordinary deconvolution methods could not be used since the system contained a nonlinear component, hence a modification of the Verotta *et al*. deconvolution method was developed [84, 85].

Bioavailability for the eflornithine enantiomers was estimated by integrating the individual systemic input rate-time profiles up to the last observation for each individual up 27 hours for the highest dose (3000 mg/kg).

3.3.7 Model validation

The model selection was based on mechanistic plausibility, parameter estimate precision, the objective function value (OFV), diagnostic plots for goodness-of-fit (GOF) and visual predictive check (VPC). For comparison of two nested models, differing by one degree of freedom, a decrease in OFV of 3.84 when using the First Order Condition Estimation method (FOCE)

suggests that the model with the lowest OFV is statistically superior ($P < 0.05$) [80]. A drop of 6.63 in OFV implies a statically superior model with a higher statistical significance ($P < 0.01$). The log-likelihood ratio test can be used to discriminate between two nested models since the OFV-difference between the full and nested model is about chi-square distributed. A bootstrap of 500 samples with the final proposed model was performed to assess parameter precision in terms of relative standard error (%RSE). The individual model parameter estimates were obtained as empirical Bayes estimates, inter-individual variability for model parameters, CL, V_c, V_t, Q, was assessed assuming a log-normal distribution. The residual error was quantitated by a proportional error model.

3.4 Paper IV – Eflornithine stereoselective extent of absorption

3.4.1 Experimental *in vivo* design

The modelling of *in vivo* pharmacokinetics presented here is based on the data generated in Paper III, hence the *in vivo* study design and methods are described in chapter 3.3.1-3.3.3.

3.4.2 Ussing chamber *in vitro* permeability assay

The present Ussing chamber assay was modified from the original method described by Ussing in 1951 [86–90]. The present Ussing chamber set-up was adapted for the rat.

Male, Sprague-Dawley, rats were sedated by inhalation of isofluran (Forene; Abbot Scandinavia AB, Solna, Sweden), the small intestine was excised by blunt dissection and transferred to ice-cold Krebb's-bicarbonate Ringer solution (KBR). The KBR solution consisted of 108 mM NaCl, 4.7 mM KCl, 1.8 mM Na_2HPO_4, 0.6 mM KH_2PO_4, 1.2 mM $MgSO_4$, 11.5 mM glucose (Scharlau, Barcelona, Spain), 16 mM $NaHCO_3$, 1.2 mM $CaCl_2$ (Sigma-Aldrich, St. Louis, MO, USA), 4.9 mM Na-pyruvate, 5.4 mM fumarate (Acros Organics, Geel, Belgium) and 4.9 mM L-glutamate (Alfa Aesar, Ward Hill, MA, USA) were dissolved in deionized water prepared by a Milli-Q deionizing water system (Millipore, Bedford, MA, USA). The KBR was constantly bubbled with carbogen gas (O_2/CO_2, 95/5%, AGA Gas, Lidingö, Sweden).

All fecal matter was flushed out of the intestine with ice-cold KBR and the segment was rested for 45 minute
s in ice-cold KBR under constant bubbling with carbogen gas.

About three centimetre long segments of the intestine were cut and care was taken to avoid the Peyer's patches. The segment-tube was opened along the mesenteric border and fixated to an ice-cold needle patch submerged in KBR solution. Remaining adipose tissue was removed and the serous muscle membrane was peeled off by hand. The segmented was then mounted in the Ussing chamber as a flat sheet between the two compartments.

The Ussing chamber system consisted of four vertical chambers (Warner Instruments, Hamden CT, USA) with a 5×24 mm oblong exposure area of 1.15 cm^2. The diffusion chambers were mounted between water jackets for circulation of warm water to maintain a constant temperature in the chambers of 37°C.

A set of electrodes were mounted on either side of the membrane in the chambers. Ag/AgCl reference electrodes (REF 201, Red Rod, Radiometer analytical, Cadex, France) submerged in saturated 3 M KCl-solution were connected to the chambers via Agar/NaCl bridges. The bridges were PE-200 tube filled with a 6% (weight/volume) of agar in a 0.9% (weight/volume) saline solution, and placed close on each side to the membrane. Platinum electrodes, plus and minus, were placed adjacent to the membrane on either side in the chamber. The electrodes were connected to a 4-channel diffusion chamber measurement system (UCC-Labs 401, UCC-labs AB, Mölndal, Sweden) and monitored the electrical parameters: resistance (R), potential difference (PD) and short circuit current (SCC). Data was collected using UCC-labs measurement software recording every 30 seconds.

Racemic eflornithine hydrochloride was dissolved in KBR at concentrations of 1, 2, 5, 10, 25 mM. ^{3}H-propranolol and ^{14}C-mannitol (5 µL of each) were added to the donor compartment solution to investigate paracellular and transcellular permeability [88]. Samples were taken from the receiver compartment at times 0, 2, 30, 60, 90, 120, 150, 180 minutes and replaced with an equal volume of KBR solution. Samples from the donor compartment were taken at 0, 60, 120, 180 minutes.

L- and D-eflornithine were quantitated separately in KBR solution using the aforementioned bioanalysis method [46]. Samples did not require protein precipitation and were therefore directly injected into the HPLC. A Jasco 821-FL spectrofluorometer (Jasco, Oklahoma, USA) was used for increased sensitivity.

The total radioactivity for each ^{3}H-propranolol and ^{14}C-mannitol were measured in each sample. A 100 µL sample was transferred to a plastic vial and mixed with 8 mL of scintillation fluid (Optisafe Hisafe 2, Perkin Elmer, USA). The disintegrations per minute (DPM) for both the ^{3}H- and the ^{14}C- were measured separately for six minutes using a liquid scintillation analyser (Tri-carb 2800 TR, Perkin Elmer, Downers Grove, IL, USA).

The apparent permeability over the rat intestine for L- and D eflornithine separately, ^{3}H-propranolol and ^{14}C-mannitol was derived using equation 12.

3.4.3 Simultaneous modelling of IV and PO eflornithine data

Simultaneous modelling of the oral and intravenous plasma concentration-time profiles for the separate eflornithine enantiomers was done using a modification of the model proposed in Paper III and chapter 3.3.6. The oral absorption of eflornithine in the rat was described by two separate routes, one stereoselective and one non-stereoselective (Figure 7).

The modelling procedure, validation and discrimination were done similar to previously described in chapter 3.3.6-3.3.7.
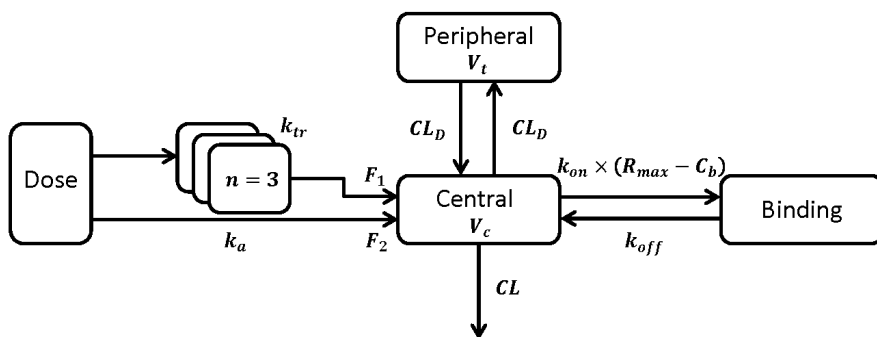

Figure 7. The semi-mechanistic model describing the oral absorption, distribution and elimination of eflornithine enantiomers in the rat. V_c and V_t are the volumes of distribution in the central and peripheral compartments, respectively. CL_D is the distribution clearance and CL is the systemic elimination clearance. C_b is the concentration in the binding compartment, k_{on} is the binding rate constant, k_{off} the dissociation rate constant and R_{max} the total amount binding target. F_1 and F_2 is the extent of absorption from each respective route and k_a is the first order absorption rate constant, and k_{tr} is the transfer rate constant. n is the number of transit compartments in that route of absorption.

Several approaches to model the oral absorption were investigated and the approach with two parallel absorption routes did adequately well describe the separate absorption profiles of eflornithine enantiomers. In one approach, the number of transit compartments was modelled as a separate parameter, however delivering a similar number, and not significantly improving the

model fit, wherefore that approach was omitted in favour of the fixed number as presented in the proposed model [91].

A proportional residual error model was used and the individual parameter estimates were obtained as empirical Bayes estimates and a log-normal distribution was assumed for the inter-individual variability of parameter estimates CL, CL_D, V_c, V_t, R_{max}, k_{on}, k_{off}, k_a, k_{tr}, F_1 and F_2.

3.5 Paper V– Eflornithine pharmacodynamics in HAT patients

3.5.1 Study design and characteristics

Data from three previously published clinical trials was collected. The treatment outcome was failure or disease/drug related death considered as an event and data was investigated in a time-to-event (TTE) modelling approach. In the investigated clinical trials, there were three different eflornithine-based treatments that were evaluated, intravenous eflornithine monotherapy, oral eflornithine monotherapy and nifurtimox-eflornithine combination treatment (NECT) [38, 7, 14]. The study characteristics are summarized below (Table 2).

Table 2. Study characteristics for each of the included studies in the analysis.

	Route	Dose [mg/kg]	Daily doses	Days		Bw [kg]	Total dose [gram]	Follow -up [months]
Eflornithine	IV	100/150[a]	4	14	672	46[c]	258	12
Eflornithine	PO	100/125[b]	4	14	24	51	333[e]	12
NECT	IV	200	2	7	551	50[d]	140	12

[c]Children below 12 years received a higher dose. [b]Two oral doses were investigated in the study. [c]Based on the complete cohort n = 1055. [d]Bodyweight is not known and a median weight of 50 kg is assumed. [e]The median total dose administered in this study was 333 g.

Intravenous eflornithine monotherapy

There were a total of 1055 patients with confirmed late-stage HAT included in the trial [14]. The trial was conducted in southern Sudan and the patients were followed for up to 39 months after treatment, the study was conducted between the years 2001 and 2002. In the present investigation data up to 12 months was used. All patients received a standard treatment of intravenous eflornithine monotherapy at 100 mg/kg QID for 14 days; a sub-group of 96 children received a higher eflornithine dose of 150 mg/kg QID. A total of 533

patients were followed for at least for 25 months and 672 for at least 12 months and 924 patients had any follow up. 68 patients with events were recorded during the 25 month follow-up and 28 were observed up to 12 months after treatment. The median bodyweight in the whole study population was 46 kg.

Oral eflornithine monotherapy

A clinical trial on oral eflornithine was conducted in 24 patients in the Côte d'Ivoire between the years 2000 and 2002 [38]. All patients had confirmed late-stage *T.b gambiense* sleeping sickness. The study population was divided into two dose groups, receiving 100 or 125 mg/kg QID oral eflornithine solution for fourteen days. The patients were followed for a total of 12 months after treatment, but assessed at 1, 3, 6, 9 and 12 months after finished treatment. The median bodyweight in the population was 51 kg.

Nifurtimox–eflornithine combination treatment

A total 551 late-stage HAT patients treated with NECT were followed for at least 12 months after treatment [7]. The clinical trial was multicentre where data was collected from 22 different centres in 9 countries and conducted between the years 2010-2011. With NECT, eflornithine is given intravenously at a dose of 200 mg/kg BID for 7 days in combination with oral nifurtimox at 15 mg/kg TID 10 days. There were 17 reported treatment failures in the 12 months follow up.

All three clinical trials were conducted in HAT endemic areas in central and western Africa and included only patients with confirmed late-stage HAT. Treatment failure in the present analysis was defined as drug or disease related deaths, and recurrent HAT infection with CSF manifestation. Self-evaluation was used in some cases for patients in good health. Children under 12 years old, although receiving a higher daily dose than adults, were included in the present analysis since the generally lower bodyweight would result in a similar total eflornithine dose. Total eflornithine dose was used as time-constant covariate for treatment outcome in the present investigation.

3.5.2 Pharmacodynamic data analysis

The time to event in each of the investigated clinical trials was modelled using NONMEM version 7.12 and model files were handled in R based programs Xpose4, PsN version 3.5.3 and Piraña version 2.6.1 [80, 81, 82, 83] The present approach has previously been applied for other diseases [71, 92–94, 95].

The time to an event was coded as a dichotomous response (0 = no event and 1 = event), no observed event until the end of the follow-up was

regarded as survival (right censoring). The survival function (Equation 16) was described using a, time varying, Weibull distribution for hazard; however fixing the shape (γ) to 1 reduces the function to exponential hazard function assuming a time-constant hazard.

$$S(t) = \Pr(T > t) = \exp\left(-Ln2\left(\frac{t}{\varphi}\right)^{\gamma}\right) \qquad \text{(Eq. 16)}$$

where S(t) is the survival function, φ is hazard for an event and γ is the Weibull shape parameter.

The probability density function p(t) (Equation 17) describes the probability for an event during the observation period

$$p(t) = \Pr(t = t) = Ln2 \times \frac{\gamma}{t} \times \left(\frac{t}{\varphi}\right)^{\gamma} \times \exp\left(-Ln2 \times \left(\frac{t}{\varphi}\right)^{\gamma}\right) \qquad \text{(Eq. 17)}$$

The time constant inhibitory effect of treatment was implemented as a sigmoid I_{max} exposure response model for the drug effect:

$$\varphi = BASE \times \left(1 - \frac{I_{max} \times DOSE^n}{ID_{50}{}^n + DOSE^n}\right) \qquad \text{(Eq. 18)}$$

where φ is the hazard for an event when considering the dose effect, BASE is the estimated baseline hazard without treatment effect, ID_{50} is the dose that generates a 50% reduction in hazard and DOSE in the total eflornithine dose administered in each study and included as a time constant covariate, Imax and the sigmoidicity factor (n) were assumed to be 1.

Maximum likelihood estimates of parameters were obtained using first order conditional estimation (FOCE) and Laplacian estimation method and goodness of fit for different models was evaluated using the objective function value (OFV). Model evaluation was based on the OFV and precision of parameter estimates. Bootstrapping was performed with the final model to assess parameter precision using 1000 resampled datasets. The final bootstrap parameters were used for simulation (n = 200) with the selected model to obtain the visual predictive check.

4 RESULTS

4.1 Paper I – Synthesis of eflornithine derivatives

The structures of the synthesized derivatives were confirmed by NMR and MS. The exemplified prodrug candidate (Figure 5) was synthesized at a yield of 86%.

In vivo pharmacokinetics

There were no or only minor quantities of eflornithine detected in plasma samples from rat after oral administration of any of the prodrug candidates. However, after oral administration of eflornithine *per se* quantities in plasma were in accordance with previous observations.

Anti–trypanosomal activity screen

The eflornithine ethyl ester (Figure 5) had a similar anti-trypanosomal activity to eflornithine, with IC_{50} values of 32 and 36 µM respectively. One of the investigated compounds, compound 10, had an IC_{50} about ten-fold lower. All other investigated compounds were less potent in the present investigation.

4.2 Paper II – Deficient eflornithine exposure *in vivo*

Physicochemical properties for each of the investigated prodrug candidates were predicted *in silico*, and predictions are summarized in the table below (Table 3). The number of hydrogen bond donors and the topological surface area were used for predictions of fraction absorbed ($F_A\%$) as implemented in the SimCYP software.

In vivo pharmacokinetics

The eflornithine enantiomers were separately quantitated in rat plasma after oral administration to the rat, and full plasma concentration-time profiles were generated (Figure 3, Paper II).

Table 3. Predicted physicochemical properties for each of the prodrug candidates and eflornithine.

Compound	Molecular weight [g/mol]	cLogP	HBD	PSA [$\mathring{A}^2$]	F_A [%]
Eflornithine	236.6	-0.82	3	89.3	44
CD1	246.7	0.41	2	78.3	74
CD2	274.2	0.95	3	92.4	41
CD3	324.3	0.16	4	113	16
CD4	360.4	3.67	3	102	35
CD5	287.3	-0.35	3	105	32
CD6	316.4	0.99	3	102	35
CD7	238.3	-0.33	3	92.4	41
CD8	286.3	0.81	3	92.4	41
CD9	304.4	1.38	5	98.7	12
CD10	224.2	-1.08	3	92.4	41

cLogP, the calculated logarithm of the partition coefficient; HBD, Hydrogen bond donors; PSA, Topological surface area; FA%, percentage of fraction absorbed. FA% was predicted based on HBD and TPSA using SimCYP.

In accordance with observations in Paper I, no or only low quantities of the prodrug metabolite eflornithine were observed in plasma after oral administration of any of the prodrug candidates to the rat.

In vitro microsomal incubations

The protein concentrations in the two batches of rat liver microsomes were slightly different, at 25.3 and 33.8 mg/mL respectively. The first-order rate constant for simultaneous depletion and formation of CAPS and CAP was estimated at 0.84 µmol/hr (n = 3, RSE = 21%) and for PA into PABA: 0.60 µmol/hr (n = 3, RSE = 22%) at an initial incubation concentration of 1000 and 100 µM respectively.

The investigated prodrug candidates were however not metabolised into eflornithine in rat liver microsomes, small but negligible eflornithine quantities were observed in phosphate buffer after incubation with candidate CD6 only.

In vitro apparent permeability

The apparent Caco-2 permeability for the investigated prodrug candidates was similar or lower to that of eflornithine (Table 3, Paper II). Mean P_{app} for ^{14}C-Mannitol was calculated to 9.01×10^{-6} cm/s. The oral fraction absorbed (F_A%) in man was predicted using the P_{app} and the fraction absorbed was predicted to be similar or lower compared to eflornithine.

4.3 Paper III – Stereoselective pharmacokinetics of eflornithine

Plasma pharmacokinetics after intravenous infusions and oral administration

The plasma concentration-time profiles after intravenous administration of
racemic eflornithine to the rat was adequately described with a three-
compartment model with linear elimination and non-linear binding to one of
the peripheral compartments (Figure 8). Enantioselective R_{max}, k_{on} and k_{off}
was suggested, however omitted since no significant improvement in the
model fit was observed. An interindividual variability (IIV) was estimated for
the following model parameters: CL, V_c, V_t and Q. Parameter estimates are
summarized in table 4.
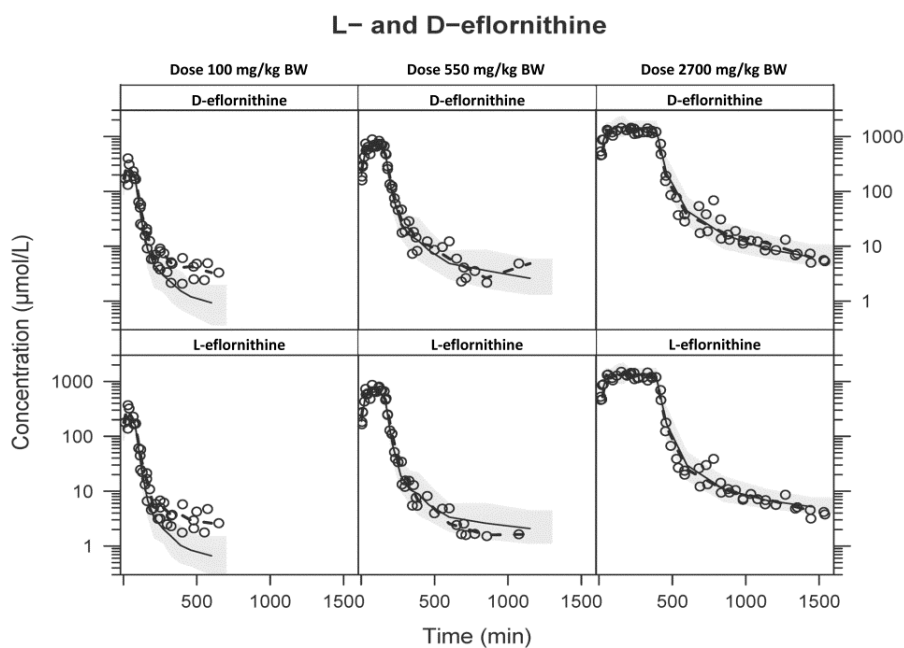
Figure 8. Visual predictive check with the 95% prediction interval for the proposed
model. The observed data is depicted as circles and the solid black line is the model
predicted median concentration with the corresponding 95% confidence interval (CI)
for the prediction in shaded grey for L- and D- eflornithine separately. The dotted
black line corresponds to the median of the observations.

Table 4. Pharmacokinetic parameter estimates for L – and D – eflornithine after intravenous infusion of racemic eflornithine hydrochloride to the rat.

PARAMETER	ABREVIATIONS	UNITS	ESTIMATE (%RSE)		IIV (CV%) (RSE%)	Shrinkage (%)
			L-DFMO	D-DFMO		
Clearance	CL	$mL \times min^{-1}$	3.36 (4.83)	3.09 (4.77)	14.1 (31.9)	2.31
Volume of the central compartment	V_c	mL	74.7 (5.73)	72.0 (5.02)	20.2 (29.6)	27.9
Volume of the peripheral compartment	V_t	mL	31.6 (5.90)	46.3 (5.72)	64.5 (31.2)	31.4
Intercompartmental clearance	Q	$mL \times min^{-1}$	0.217 (6.12)	0.274 (5.94)	71.2 (24.5)	4.7
Total binding capacity	R_{max}	µmol	73.3 (5.73)			
Binding rate constant	K_{on}	$mL \times min^{-1} \times µmol^{-1}$	0.00275 (7.98)			
Dissociation rate constant	K_{off}	min^{-1}	0.000468 (5.75)			
σ proportional residual error		%	17.7 (8.82)			7.82

Parameters are represented for the typical rat weight of 338.4 gram. IIV shows inter individual variability with the corresponding CV%. Shrinkage (η and ε) for each corresponding parameters is given as percent. %RSE, Relative Standard Error, is estimated with bootstrap (500 samples).

The mean population pharmacokinetic parameters after IV administration
was used for estimation of the input rate function of oral data (Figure 9). The
bioavailability was estimated at 30 and 59% with deconvolution for L- and
D-eflornithine respectively. Input parameters from deconvolution of oral data
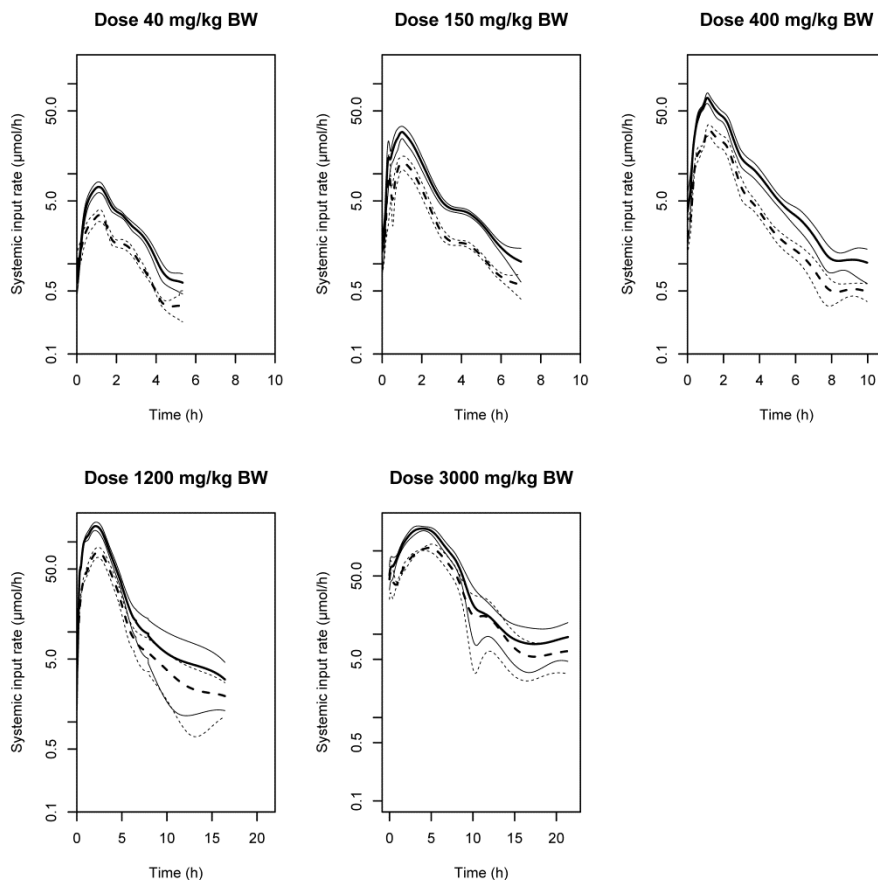are summarized in table 3, paper III.

Figure 9. Mean systemic input rate from gut versus time after oral administration of
each dose 40, 150, 400, 1200, and 3000 mg/kg of racemic eflornithine. Heavy dashed
and solid lines represent the mean input rate-time profiles for L- and D-eflornithine,
and the thin lines the corresponding 95% confidence intervals.

Faeces D – to L – eflornithine ratios

For the reference samples prepared in rat faeces, the median D:L peak area ratio was 1.03 (range: 0.98 – 1.15, n = 6), thus endogenous substances are not expected to interfere with the outcome of the samples from rats receiving eflornithine orally. In faeces samples after oral administration of eflornithine, the mean D:L peak area ratio was 0.49 ± 0.03 (± standard error; n = 11) and at range of 0.3 – 0.6. This observed D:L ratio was the inverse to what was observed in plasma, consequently more L-eflornithine remained in the gut whilst more D-eflornithine was absorbed.

Bidirectional transport in Caco–2 cells

The mean transepithelial resistance values of the Caco-2 monolayers were 255 Ω cm^2 (SD ± 16; n = 9) before the experiment and decreased to 217 Ω cm^2 after the incubations. The apparent permeability of eflornithine enantiomers was low for both the investigated concentrations, 0.75 and 12.5 mM, at 6.06×10^{-8} cm/s (SD ± 1.31) to 7.29×10^{-8} cm/s (SD ± 0.16) and 6.19×10^{-8} cm/s (SD ± 1.32) to 6.91×10^{-8} cm/s (SD ± 0.22) for L- and D-eflornithine respectively. No involvement of P-gp was observed.

4.4 Paper IV – Eflornithine stereoselective extent of absorption

Plasma pharmacokinetics after oral and IV administration

The separate plasma concentration-time profiles for L- and D-eflornithine after both oral and intravenous administration to the rat was well described using the proposed model (Figure 10) and parameter estimates are summarized in table 1, paper IV.

The stereoselective absorption was estimated jointly for the enantiomers and was modelled as two separate routes. The absorption rate constant (k_a) and transfer rate constant (k_{tr}) were estimated at 0.00568 min^{-1} (%RSE = 58.7) and 0.225 min^{-1} (%RSE = 3.12) respectively. No significant improvement in the model fit was observed when separating these two parameters for each respective enantiomer. The extent of absorption was separated for the enantiomers through modelling of a separate bioavailability for each of the proposed routes (F_1 and F_2). F_1 was estimated at 28.9% (%RSE = 8.05) and 55.9% (%RSE = 5.83), and F_2 at 3.56% (%RSE = 28.4) and 3.26% (%RSE = 30.1) for L- and D-eflornithine, respectively.
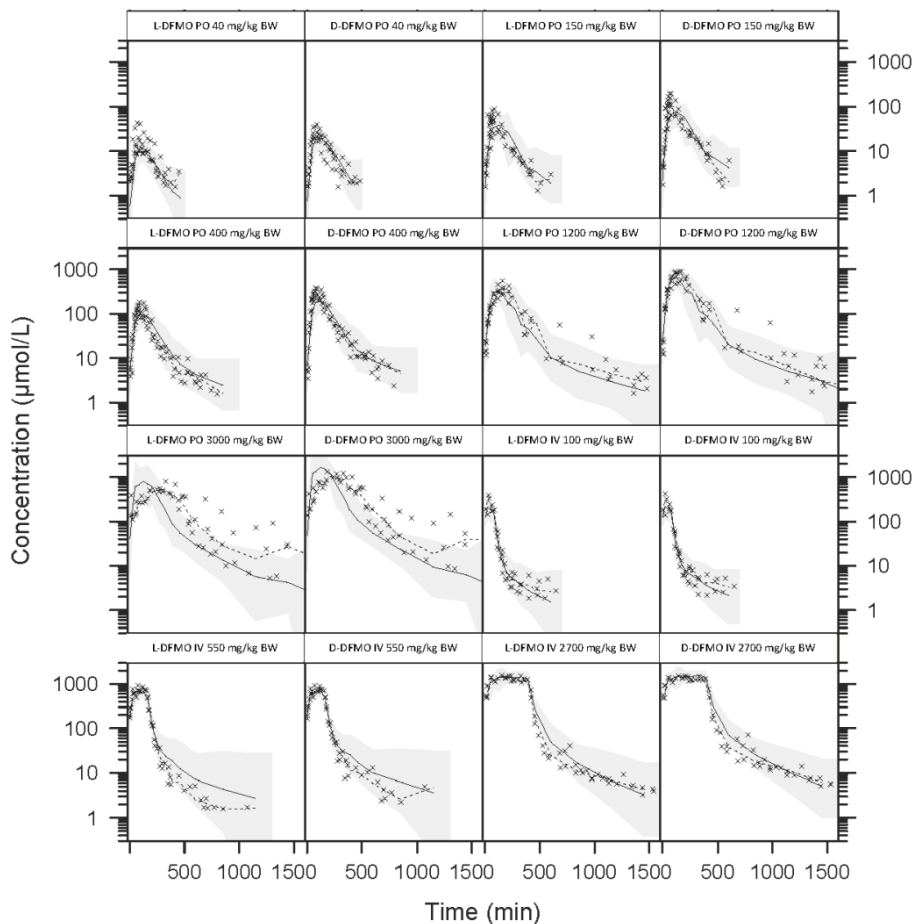
Figure 10. Visual predictive check for simultaneous modelling of L- and D-eflornithine oral and intravenous data. Grey shaded areas constitute the 95% prediction interval, (×) represent the observations, (--) represent the median of the observations and (—) the median predicted concentration.

Ussing chamber permeability

Separate apparent permeability was derived at 3.92×10^{-5} cm/s (SD ± 0.954) and 4.63×10^{-5} cm/s (SD ± 1.46), for L- and D-eflornithine respectively. There was no observed difference in eflornithine recovery in the receiver compartment. The mean trans-epithelial potential difference (PD) and short circuit current (SCC) were 5.7 mV (range: 2.7 – 11.2 mV) and 173 µA (range: 81 – 288 µA) respectively, at initiation of the experiments.

4.5 Paper V– Eflornithine pharmacodynamics in HAT patients

The selected model could adequately describe the time-to-event in the present three clinical studies with three different eflornithine-based dosage regimens. Parameter estimates and parameter precision for the baseline hazard and dose effect were generated by bootstrapping the final model 1000 times. A visual predictive check was done, using the selected model and simulating 200 times (Figure 11).
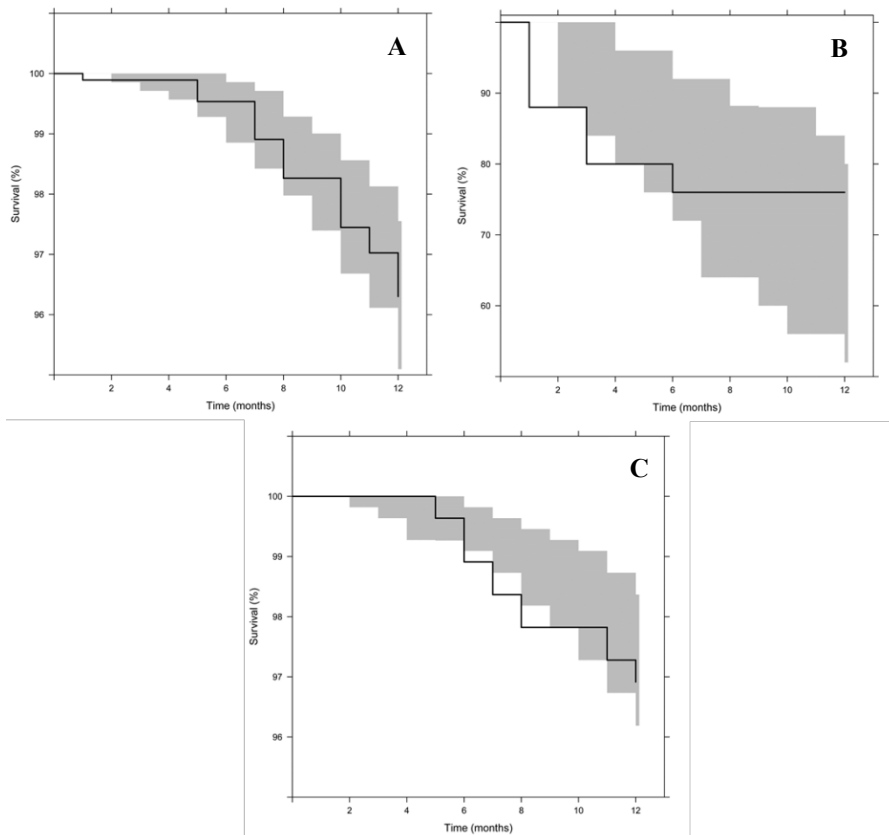

Figure 11. Shows a visual predictive check for the three separate studies. Figure 1(A) is the intravenous eflornithine monotherapy, 1(B) is the oral eflornithine monotherapy and 1(C) is the nifurtimox-eflornithine combination treatment. The solid black line represents the observed survival in the study and the grey shaded areas represent the 95% confidence interval for the model predictions, obtained from 200 simulations with the final model.

The intravenous eflornithine monotherapy and the nifurtimox combination treatment data was modeled using the Weibull hazard distribution model. For oral eflornithine, the Weibull shape parameter was fixed equal to 1, and estimated at 2.59 (95% CI = 2.56-2.63) and 1.98 (95% CI = 1.96-2.00) for intravenous eflornithine monotherapy and the combination treatment, respectively. The baseline hazard was similar in the intravenous eflornithine and the combination treatment studies at 0.0390 (95% CI = 0.0386-0.0394) and 0.0276 (95% CI = 0.0272-0.0279) 1/month, respectively. Baseline hazard was higher in the oral eflornithine study, 0.0822 (95% CI = 0.0805-0.0840) 1/month. There was a three-fold difference in the estimated ID_{50}-values between the oral and intravenous eflornithine monotherapy studies at 294 (95% CI =288-299) and 116 (95% CI = 113-120) g, respectively. The ID_{50}-value for the combination treatment was estimated at 54.4 (95% CI = 53.5-55.3) g.

5 DISCUSSION

Based on the present investigation it can be concluded that there were no or only low quantities of eflornithine enantiomers after oral administration to the rat of any of the investigated prodrug candidates. This absence of eflornithine in plasma required further study to investigate if the cause was inadequate gastrointestinal absorption or metabolic stability. Based on the results in the present thesis it could be concluded that the probable cause was high metabolic stability. This confirms, for some of the compounds, our previous observations and the stability previously reported by others regarding eflornithine based derivatives [96, 97]. The investigated compounds herein had also a low permeability over Caco-2 cell monolayers with subsequent expected low fraction absorbed, this alone could not however explain the absence of eflornithine systemically and is contradictory to the *in silico* predictions based on physicochemical properties.

The rat is generally considered to have a higher esterase activity compared to man and with this perspective the stability of the investigated eflornithine ethyl ester is somewhat surprising. In the present thesis it is hypothesized that the stability observed for all prodrug candidates could be caused thru bond stabilization by the electronegative fluoride groups of the eflornithine molecule [98]. Other plausible explanations for the observed metabolic stability may be that the candidates undergo conformational changes or steric hindrance that protects the ester or amide bond from being cleaved.

There was a possible toxic effect by the derivatives on the Caco-2 cells, exposed in the high permeability of the probe substance ^{14}C-mannitol. The impact of this toxic effect has not further been investigated.

Anti-trypanosomal effect was investigated for selected derivatives and the pharmacological activity was comparable to eflornithine *per se* or lower. However, the stable eflornithine ethyl ester candidate (CD1) showed an activity similar to eflornithine and a higher predicted fraction absorbed, that may inspire continued investigation. It can be hypothesized that the metabolic stability could increase the long-term exposure of both CD1 and eflornithine, thus facilitating an oral dosage regimen.

The oral non-stereoselective bioavailability of eflornithine has been reported to be about 54% in man after administration of racemic mixture [37]. Increasing the *in vivo* exposure can be challenging considering the already relatively high bioavailability and the dose limiting side effect associated with higher doses [38]. In the recently implemented NECT-combination, the total dose and duration of the eflornithine treatment could be reduced due to the suggested additive effect when combining eflornithine

with nifurtimox. This was possible under the assumption that the total dose administered (daily dose multiplied by the treatment duration) is the primary driver of pharmacological effect. A relatively low increase in the total exposure of active drug, eflornithine and/or active derivative could open possibilities for an oral dosage regimen.

A key component to the development of oral an eflornithine treatment is to understand the implications of stereoselectivity on the pharmacokinetics and pharmacodynamics. The stereoselective *in vivo* eflornithine pharmacokinetics in the rat was described in paper III. Several models were investigated to describe plasma concentration-time profiles of the eflornithine enantiomers. A reduction in the volume of distribution with increasing dose suggested a target-mediated approach. The model proposed in paper III was a modification of a previously described model for TMDD [69, 70]. Eflornithine enantiomers had similar T_{max}-values after oral administration, which suggested that the enantiomers have similar rates of absorption from the gastrointestinal tract. Separate bioavailability for the eflornithine enantiomers were estimated by deconvolution showing that L- eflornithine had a 50% lower bioavailability compared to D-eflornithine. Several possible explanations for this difference could be excluded, *e.g.* interconversion and presystemic metabolism. However, a more mechanistic approach to describe the oral absorption was needed. In paper IV a semi-mechanistic absorption model was coupled to the pharmacokinetic model proposed in paper III. Several different approaches to model the oral absorption were taken, and the finally proposed model consisted of two separate absorption routes, one stereoselective described with a number of transit compartments and one non-stereoselective route. The bioavailability was modelled separately for the two routes. The modelling results further supported prior observations that the absorption rate was similar for both enantiomers however differing in their extent of absorption. A proposed explanation for this stereoselective difference in the extent of absorption was the formation of a chemical complex in the gut prior to absorption. The hypothesized complex could consist of two L-eflornithine enantiomers binding each other or two L-eflornithine binding to one D-eflornithine. The stereoselectivity and slower onset of the second route may then describe the absorption or dissolution of the chemical complex.

Stereoselective apparent permeability was investigated over both Caco-2 cell monolayers and in the Ussing chamber using excised rat intestine. The density of the Caco-2 cells may underestimate the permeability of small and hydrophilic compounds like eflornithine which motivated investigation also in the more physiological *in vitro* system, the Ussing chamber [60]. The apparent permeability was similar for both enantiomers over Caco-2 cell

monolayer and in the Ussing chamber, which suggests that the putative complexation does not occur outside the gastrointestinal tract.

Administering the eflornithine enantiomers separately could possibly give more information about the mechanisms. If the suggested chemical complex was constituted of two L-enantiomers binding to one D-enantiomer, the administration of optically pure eflornithine may limit this interaction, thus overcoming the stereoselective absorption.

The assessment of the eflornithine pharmacodynamics in paper V suggests that it is foremost the L-enantiomer that elicits the pharmacological effect in HAT patients, since it may be speculated that the three-fold difference in ID_{50} between oral and intravenous eflornithine monotherapy was caused by the L-eflornithine bioavailability of 30%. The increased potency in the combination treatment with nifurtimox may improve efficacy enough to motivate a continued investigation of an oral eflornithine dosage regimen.

6 CONCLUSION

The most important conclusion in the present thesis is the novel understanding of the enantioselective absorption mechanism motivates further investigations into the pharmacokinetics and pharmacodynamics of the eflornithine enantiomers separately. Other specific conclusions were:

- The pharmacokinetic modelling together with the experimental work collectively improved the understanding of hurdles and opportunities to developing an oral eflornithine based treatment. Both approaches render valuable information to the on-going strive for improved treatment alternatives against HAT.

- The investigated prodrug candidates exhibited no increase in permeability and were metabolically stable without improving plasma concentrations of eflornithine. This was suggestedly caused by electronegative interactions of conformational changes to the eflornithine molecule rendering the ester and amide bonds less accessible to metabolising enzymes.

- In the rat, oral bioavailability of L-eflornithine is 50% lower compared to D-eflornithine which is expected to be of significant clinical importance for oral treatment bearing in mind the difference in potency.

- The observed enantioselective difference in oral bioavailability was caused by a difference in the extent of absorption but absorption rates were similar for both enantiomers.

- A chemical complex forming in the GI tract could explain the different extent of absorption between the eflornithine enantiomers.

- L-eflornithine was suggested to be mainly responsible for the pharmacological effect in HAT-patients based on the 1:3 ratio in ID_{50} between oral and intravenous eflornithine monotherapy.

ACKNOWLEDGEMENT

Christine Ahlström, for fantastic conference hang and being a great travel companion.

My thesis project students Erik Andersson and Helena Norling for valuable inputs.

This work was made a lot easier by great friends and family:

Anders Björklund and Sofia Friberg for all the laughs we have shared and for your help and support when I needed it the most. Life outside science has been brighter in your company!

Åsa and Patrik Hyberg, Maria Wideqvist and Martin Sandberg, Annasara Hansson, Elin Nilsson and Therese Lidhamn for being great friends, supportive and for believing in me. We have shared much fun over the years while studying, partying, travelling, skiing and celebrating midsummer.

Erik Hellervik, for being a wonderful friend and very encouraging.

Theunis and Anke Cloete for taking care of me when I was visiting South Africa and for the adventures and fun times spent together.

Mom and Dad for all the support and encouragement over the years. You have always been there for me, giving love and a helping hand when needed. My favourite sister Malin, thank you for cheerful pep and support. Sir Lancelot for comforting times…

The Amilon clan for welcoming me into the family and for your support.

Finally, my darling Sofia for being the most wonderful thing in my life! Your support and belief in me has made it all possible.

"Perhaps he know, as I did not, that the Earth was made round so that we would not see too far down the road." *Karen Blixen*

REFERENCES

1.   L.Z. Benet (1984) Pharmacokinetics: Basic Principles and Its Use as a Tool in Drug Metabolism. In: Horning JR, Mitchell MG (eds) Drug Metabolism and Drug Toxicity. Raven Press, New York NY USA, pp 199–211

2.   Brun R, Blum J, Chappuis F, Burri C (2010) Human African trypanosomiasis. Lancet 375:148–59

3.   Simarro PP, Jannin J, Cattand P (2008) Eliminating human African trypanosomiasis: where do we stand and what comes next? PLoS medicine 5:e55

4.   Malvy D, Chappuis F (2011) Sleeping sickness. Clinical microbiology and infection : the official publication of the European Society of Clinical Microbiology and Infectious Diseases 17:986–95

5.   Simarro PP, Diarra A, Ruiz Postigo J a, Franco JR, Jannin JG (2011) The human African trypanosomiasis control and surveillance programme of the World Health Organization 2000-2009: the way forward. PLoS neglected tropical diseases 5:e1007

6.   Priotto G, Kasparian S, Ngouama D, Ghorashian S, Arnold U, Ghabri S, Karunakara U (2007) Nifurtimox-eflornithine combination therapy for second-stage *Trypanosoma brucei gambiense* sleeping sickness: a randomized clinical trial in Congo. Clinical infectious diseases : an official publication of the Infectious Diseases Society of America 45:1435–42

7.   Franco J, Pere S (2012) Monitoring the use of nifurtimox-eflornithine combination therapy (NECT) in the treatment of second stage gambiense human African trypanosomiasis. Research and Reports in Tropical Medicine 93

8.   Kennedy PGE (2008) The continuing problem of human African trypanosomiasis (sleeping sickness). Annals of neurology 64:116–26

9.   Krafsur ES (2009) Tsetse flies: genetics, evolution, and role as vectors. Infection, genetics and evolution : journal of molecular epidemiology and evolutionary genetics in infectious diseases 9:124–41

10.   Maudlin I, Welburn SC, Milligan PJ (1998) *Trypanosome* infections and survival in tsetse. Parasitology 116 Suppl:S23–8

11.   Van Nieuwenhove S, Schechter PJ, Declercq J, Boné G, Burke J, Sjoerdsma
        A (1985) Treatment of gambiense sleeping sickness in the Sudan with oral
        DFMO (DL-alpha-difluoromethylornithine), an inhibitor of ornithine
        decarboxylase; first field trial. Transactions of the Royal Society of Tropical
        Medicine and Hygiene 79:692–8

12.   Vincent IM, Creek D, Watson DG, Kamleh M a, Woods DJ, Wong PE,
        Burchmore RJS, Barrett MP (2010) A molecular mechanism for eflornithine
        resistance in African *trypanosomes*. PLoS pathogens. doi:
        10.1371/journal.ppat.1001204

13.   Vincent IM, Creek D, Watson DG, Kamleh M a, Woods DJ, Wong PE,
        Burchmore RJS, Barrett MP (2010) A molecular mechanism for eflornithine
        resistance in African *trypanosomes*. PLoS pathogens 6:e1001204

14.   Priotto G, Pinoges L, Fursa IB, Burke B, Nicolay N, Grillet G, Hewison C,
        Balasegaram M (2008) Safety and effectiveness of first line eflornithine for
        Trypanosoma brucei gambiense sleeping sickness in Sudan: cohort study.
        BMJ (Clinical research ed) 336:705–8

15.   Vodnala SK, Ferella M, Lundén-Miguel H, et al (2009) Preclinical
        assessment of the treatment of second-stage African trypanosomiasis with
        cordycepin and deoxycoformycin. PLoS neglected tropical diseases 3:e495

16.   Brun R, Schumacher R, Schmid C, Kunz C, Burri C (2001) The phenomenon
        of treatment failures in Human African Trypanosomiasis. Tropical medicine
        & international health : TM & IH 6:906–14

17.   Priotto G, Fogg C, Balasegaram M, Erphas O, Louga A, Checchi F, Ghabri
        S, Piola P (2006) Three drug combinations for late-stage *Trypanosoma
        brucei gambiense* sleeping sickness: a randomized clinical trial in Uganda.
        PLoS clinical trials 1:e39

18.   Lutje V, Seixas J, Kennedy A (2010) Chemotherapy for second-stage Human
        African trypanosomiasis. Cochrane Database Syst Rev CD006201

19.   Stich A, Abel PM, Krishna S (2002) Human African trypanosomiasis. BMJ
        (Clinical research ed) 325:203–6

20.   Kotthaus J, Kotthaus J, Schade D, Schwering U, Hungeling H, Müller-Fielitz
        H, Raasch W, Clement B (2011) New prodrugs of the antiprotozoal drug
        pentamidine. ChemMedChem 6:2233–42

21.   Alirol E, Schrumpf D, Amici Heradi J, Riedel A, De Patoul C, Quere M, Chappuis F (2012) Nifurtimox-Eflornithine Combination Therapy for Second-Stage Gambiense Human African Trypanosomiasis: Medecins Sans Frontieres Experience in the Democratic Republic of the Congo. Clinical infectious diseases : an official publication of the Infectious Diseases Society of America 56:195–203

22.   Blum J, Nkunku S, Burri C (2001) Clinical description of encephalopathic syndromes and risk factors for their occurrence and outcome during melarsoprol treatment of human African trypanosomiasis. Tropical medicine & international health : TM & IH 6:390–400

23.   Pépin J, Milord F, Khonde AN, Niyonsenga T, Loko L, Mpia B, De Wals P (1995) Risk factors for encephalopathy and mortality during melarsoprol treatment of *Trypanosoma brucei gambiense* sleeping sickness. Transactions of the Royal Society of Tropical Medicine and Hygiene 89:92–7

24.   Nok AJ (2003) Arsenicals (melarsoprol), pentamidine and suramin in the treatment of human African trypanosomiasis. Parasitology research 90:71–9

25.   Chappuis F (2007) Melarsoprol-free drug combinations for second-stage Gambian sleeping sickness: the way to go. Clinical infectious diseases : an official publication of the Infectious Diseases Society of America 45:1443–5

26.   WHO (1998) Control and surveillance of African trypanosomiasis. Report of a WHO Expert Committee. World Health Organization technical report series 881:I–VI, 1–114

27.   Bacchi CJ, Nathan HC, Hutner SH, McCann PP, Sjoerdsma a (1980) Polyamine metabolism: a potential therapeutic target in *trypanosomes*. Science (New York, NY) 210:332–4

28.   Qu N, Ignatenko N a, Yamauchi P, Stringer DE, Levenson C, Shannon P, Perrin S, Gerner EW (2003) Inhibition of human ornithine decarboxylase activity by enantiomers of difluoromethylornithine. The Biochemical journal 375:465–70

29.   Meyskens FL, Gerner EW (1999) Development of Difluoromethylornithine (DFMO) as a Chemoprevention Agent Development of Difluoromethylornithine (DFMO) as a Chemoprevention Agent 1. 945–951

30.   Fairlamb a H, Henderson GB, Bacchi CJ, Cerami a (1987) In vivo effects of difluoromethylornithine on trypanothione and polyamine levels in bloodstream forms of *Trypanosoma brucei*. Molecular and biochemical parasitology 24:185–91

31.   Griffin CA, Slavik M, Chien SC, Hermann J, Thompson G, Blanc O, Luk GD, Baylin SB, Abeloff MD (1987) Phase I trial and pharmacokinetic study of intravenous and oral alpha-difluoromethylornithine. Investigational new drugs 5:177–86

32.   Bitonti AJ, McCann PP, Sjoerdsma A (1986) Necessity of antibody response in the treatment of African trypanosomiasis with alpha-difluoromethylornithine. Biochemical pharmacology 35:331–4

33.   Balasegaram M, Young H, Chappuis F, Priotto G, Raguenaud M-E, Checchi F (2009) Effectiveness of melarsoprol and eflornithine as first-line regimens for gambiense sleeping sickness in nine Médecins Sans Frontières programmes. Transactions of the Royal Society of Tropical Medicine and Hygiene 103:280–90

34.   Balasegaram M, Harris S, Checchi F, Ghorashian S, Hamel C, Karunakara U (2006) Melarsoprol versus eflornithine for treating late-stage Gambian trypanosomiasis in the Republic of the Congo. Bulletin of the World Health Organization 84:783–91

35.   Priotto G, Kasparian S, Mutombo W, et al (2009) Nifurtimox-eflornithine combination therapy for second-stage African *Trypanosoma brucei gambiense* trypanosomiasis: a multicentre, randomised, phase III, non-inferiority trial. Lancet 374:56–64

36.   Milord F, Loko L, Ethier L, Mpia B, Pépin J (1993) Eflornithine concentrations in serum and cerebrospinal fluid of 63 patients treated for *Trypanosoma brucei gambiense* sleeping sickness. Transactions of the Royal Society of Tropical Medicine and Hygiene 87:473–7

37.   Burri C, Brun R (2003) Eflornithine for the treatment of human African trypanosomiasis. Parasitology research 90 Supp 1:S49–52

38.   Na-Bangchang K, Doua F, Konsil J, Hanpitakpong W, Kamanikom B, Kuzoe F (2004) The pharmacokinetics of eflornithine (alpha-difluoromethylornithine) in patients with late-stage *T.b. gambiense* sleeping sickness. European journal of clinical pharmacology 60:269–78

39.   Yun O, Priotto G, Tong J, Flevaud L, Chappuis F (2010) NECT is next: implementing the new drug combination therapy for *Trypanosoma brucei gambiense* sleeping sickness. PLoS neglected tropical diseases 4:e720

40. Boiani M, Piacenza L, Hernández P, Boiani L, Cerecetto H, González M, Denicola A (2010) Mode of action of nifurtimox and N-oxide-containing heterocycles against *Trypanosoma cruzi*: is oxidative stress involved? Biochemical pharmacology 79:1736–45

41. Bliss C (1939) The Toxicity of Poisons Applied Jointly. Annals of Applied Biology 26:585–615

42. Fairlamb AH (2003) Chemotherapy of human African trypanosomiasis: current and future prospects. Trends in Parasitology 19:488–494

43. Sanderson L, Dogruel M, Rodgers J, Bradley B, Thomas SA (2008) The blood-brain barrier significantly limits eflornithine entry into *Trypanosoma brucei brucei* infected mouse brain. Journal of neurochemistry 107:1136–46

44. Haegele KD, Alken RG, Grove J, Schechter PJ, Koch-Weser J (1981) Kinetics of alpha-difluoromethylornithine: an irreversible inhibitor of ornithine decarboxylase. Clinical pharmacology and therapeutics 30:210–7

45. Jansson R, Malm M, Roth C, Ashton M (2008) Enantioselective and nonlinear intestinal absorption of eflornithine in the rat. Antimicrobial agents and chemotherapy 52:2842–8

46. Jansson-Löfmark R, Römsing S, Albers E, Ashton M (2010) Determination of eflornithine enantiomers in plasma by precolumn derivatization with o-phthalaldehyde-N-acetyl-L-cysteine and liquid chromatography with UV detection. Biomedical chromatography : BMC 24:768–73

47. Rowland M, Tozer TN (2009) Clinical Pharmacokinetics and Pharmacodynamics: concepts and applications. 29

48. Balant L (1991) Is there a need for more precise definitions of bioavailability? Conclusions of a consensus workshop, Munich, September 9, 1989; under the patronage of the F.I.P. European journal of clinical pharmacology 40:123–6

49. FDA (2012) Code of Federal Regulations Title 2, Part 320.1 general definitions.

50. Ungell A-L (1997) In Vitro Absorption Studies and Their Relevance to Absorption from the GI Tract. Drug Development and Industrial Pharmacy 23:879–892

51. Lennernäs H (1998) Human intestinal permeability. Journal of pharmaceutical sciences 87:403–10

52.   Shugarts S, Benet LZ (2009) The role of transporters in the pharmacokinetics
      of orally administered drugs. Pharmaceutical research 26:2039–54

53.   Suzuki H, Sugiyama Y (2000) Role of metabolic enzymes and efflux
      transporters in the absorption of drugs from the small intestine. European
      journal of pharmaceutical sciences : official journal of the European
      Federation for Pharmaceutical Sciences 12:3–12

54.   Paine MF, Khalighi M, Fisher JM, Shen DD, Kunze KL, Marsh CL, Perkins
      JD, Thummel KE (1997) Characterization of interintestinal and
      intraintestinal variations in human CYP3A-dependent metabolism. The
      Journal of pharmacology and experimental therapeutics 283:1552–62

55.   Thelen K, Dressman JB (2009) Cytochrome P450-mediated metabolism in
      the human gut wall. The Journal of pharmacy and pharmacology 61:541–58

56.   Stenberg P, Luthman K, Artursson P (2000) Virtual screening of intestinal
      drug permeability. Journal of controlled release : official journal of the
      Controlled Release Society 65:231–43

57.   Swaan PW (1998) Recent advances in intestinal macromolecular drug
      delivery via receptor-mediated transport pathways. Pharmaceutical research
      15:826–34

58.   Sugano K, Kansy M, Artursson P, et al (2010) Coexistence of passive and
      carrier-mediated processes in drug transport. Nature reviews Drug discovery
      9:597–614

59.   Lennernäs H (2007) Intestinal permeability and its relevance for absorption
      and elimination. Xenobiotica; the fate of foreign compounds in biological
      systems 37:1015–51

60.   Matsson P, Bergström C a S, Nagahara N, Tavelin S, Norinder U, Artursson
      P (2005) Exploring the role of different drug transport routes in permeability
      screening. Journal of medicinal chemistry 48:604–13

61.   Adson a, Raub TJ, Burton PS, Barsuhn CL, Hilgers a R, Audus KL, Ho NF
      (1994) Quantitative approaches to delineate paracellular diffusion in cultured
      epithelial cell monolayers. Journal of pharmaceutical sciences 83:1529–36

62.   Chiba H, Osanai M, Murata M, Kojima T, Sawada N (2008) Transmembrane
      proteins of tight junctions. Biochimica et biophysica acta 1778:588–600

63.   Goodman LS, Hardman JG, Limbird LE GA (2002) Goodman and Gilman's
      the pharmacological basis of therapeutics, 10th ed. McGraw-Hill New York

64. Stella VJ (2010) Prodrugs : Some Thoughts and Current Issues. 99:4755–4765

65. Testa B MJ (2003) Hydrolysis in drug and prodrug metabolism : chemistry, biochemistry, and enzymology. 780

66. Rautio J, Kumpulainen H, Heimbach T, Oliyai R, Oh D, Järvinen T, Savolainen J (2008) Prodrugs: design and clinical applications. Nature reviews Drug discovery 7:255–70

67. Grasela TJ, Sheiner L (1991) Pharmacostatistical modeling for observational data. Journal of pharmacokinetics and biopharmaceutics 19:25–36

68. Levy G (1994) Pharmacologic target-mediated drug disposition. Clinical pharmacology and therapeutics 56:248–52

69. Mager DE, Jusko WJ (2001) General pharmacokinetic model for drugs exhibiting target-mediated drug disposition. Journal of pharmacokinetics and pharmacodynamics 28:507–32

70. Karlsson MO, Molnar V, Freijs A, Nygren P, Bergh J, Larsson R (1999) Pharmacokinetic models for the saturable distribution of paclitaxel. Drug metabolism and disposition: the biological fate of chemicals 27:1220–3

71. Cox EH, Veyrat-Follet C, Beal SL, Fuseau E, Kenkare S, Sheiner LB (1999) A population pharmacokinetic-pharmacodynamic analysis of repeated measures time-to-event pharmacodynamic responses: the antiemetic effect of ondansetron. Journal of pharmacokinetics and biopharmaceutics 27:625–44

72. Ette E, Roy A, Nandy P (2007) Population Pharmacokinetic/Pharmacodynamic Modeling of Ordered Categorical Longitudinal Data. Pharmacometrics: The Science of Quantitative Pharmacology. John Wiley & Sons, pp 655–672

73. March J (1992) March's Advanced Organic Chemistry: Reactions, Mechanisms and Structure. In: Smith MB (ed) 5th ed. Wiley & Sons, New York, pp 293–500

74. Smith PK, Krohn RI, Hermanson GT, Mallia AK, Gartner FH, Provenzano MD, Fujimoto EK, Goeke NM, Olson BJ, Klenk DC (1985) Measurement of protein using bicinchoninic acid. Analytical biochemistry 150:76–85

75. Hubatsch I, Ragnarsson EGE, Artursson P (2007) Determination of drug permeability and prediction of drug absorption in Caco-2 monolayers. Nature protocols 2:2111–9

76.   Jewell C, Ackermann C, Payne NA, Fate G, Voorman R, Williams FM (2007) Specificity of procaine and ester hydrolysis by human, minipig, and rat skin and liver. Drug metabolism and disposition: the biological fate of chemicals 35:2015–22

77.   Ashton M (1989) Hplc Determination of Chloramphenicol, Chloramphenicol Monosuccinate and Chloramphenicol Glucuronide in Biological Matrices. Journal of Liquid Chromatography 12:1719–1732

78.   Stenberg P, Norinder U, Luthman K, Artursson P (2001) Experimental and computational screening models for the prediction of intestinal drug absorption. Journal of medicinal chemistry 44:1927–37

79.   Hill AV (1910) The possible effects of the aggregation of the molecules of haemoglobin on its dissociation curves.No Title. The Journal of physiology 40:iv–vii

80.   Boeckman A, Sheiner L, Beal S (2010) NONMEM Users Guide. NONMEM Project Group, University of California 1–61

81.   Jonsson EN, Karlsson MO (1999) Xpose--an S-PLUS based population pharmacokinetic/pharmacodynamic model building aid for NONMEM. Computer methods and programs in biomedicine 58:51–64

82.   Lindbom L, Pihlgren P, Jonsson EN, Jonsson N (2005) PsN-Toolkit--a collection of computer intensive statistical methods for non-linear mixed effect modeling using NONMEM. Computer methods and programs in biomedicine 79:241–57

83.   Keizer RJ, Zandvilet AS, Huitema AD (2008) A simple infrastructure and graphical user interface (GUI) for distributed NONMEM analysis on standard network environments. Abstracts of the Annual Meeting of the Population Approach Group in Europe

84.   Verotta D (1996) Concepts, properties, and applications of linear systems to describe distribution, identify input, and control endogenous substances and drugs in biological systems. Critical reviews in biomedical engineering 24:73–139

85.   De Boor C (2001) Smoothing and least-squares approximation. In: Applied Mathematical Sciences 27 - A Practical Guide to Splines. 211–214

86.   Ussing H, Zerahn K (1951) Active Transport of Sodium as the Source of Electric Current in the Short-□circuited Isolated Frog Skin. Acta Physiologica Scandinavica 10:2056–65

87. Ungell a L, Andreasson a, Lundin K, Utter L (1992) Effects of enzymatic inhibition and increased paracellular shunting on transport of vasopressin analogues in the rat. Journal of pharmaceutical sciences 81:640–5

88. Polentarutti BI, Peterson AL, Sjöberg AK, Anderberg EK, Utter LM, Ungell AL (1999) Evaluation of viability of excised rat intestinal segments in the Ussing chamber: investigation of morphology, electrical parameters, and permeability characteristics. Pharmaceutical research 16:446–54

89. Grass GM, Sweetana SA (1988) In vitro measurement of gastrointestinal tissue permeability using a new diffusion cell. Pharmaceutical research 5:372–6

90. Artursson P, Ungell A, Löfroth J (1993) Selective paracellular permeability in two models of intestinal absorption: cultured monolayers of human intestinal epithelial cells and rat intestinal segments. Pharmaceutical research 10:1123–9

91. Savic RM, Jonker DM, Kerbusch T, Karlsson MO (2007) Implementation of a transit compartment model for describing drug absorption in pharmacokinetic studies. Journal of pharmacokinetics and pharmacodynamics 34:711–26

92. Miller R, Frame B, Corrigan B, Burger P, Bockbrader H, Garofalo E, Lalonde R (2003) Exposure-response analysis of pregabalin add-on treatment of patients with refractory partial seizures. Clinical pharmacology and therapeutics 73:491–505

93. Miller R, Ouellet D, Burger P, Corrigan BW (2005) Exposure-Response Analysis Using Time to Event Data: An Example Using Sleep Onset. Poster Population approach groupe Europe (PAGE) meeting

94. Tarning J, Chotsiri P, Jullien V, et al (2012) Population pharmacokinetic and pharmacodynamic modeling of amodiaquine and desethylamodiaquine in women with plasmodium vivax malaria during and after pregnancy. Antimicrobial agents and chemotherapy 56:5764–73

95. Kim H (2012) Pharmacometric modeling and simulation of ranitidine in human gastric acid secretion. Doctoral Thesis at the University of Minnesota Doctoral Thesis at the University of Minnesota.

96. Helena KJ, N'Da DD, Johansson CC, Breytenbach JC, Ashton M (2010) Effects of oral administration of synthesized delta-amides of eflornithine in the rat. Arzneimittel-Forschung 60:682–8

97.   Chollet C, Baliani A, Wong PE, Barrett MP, Gilbert IH (2009) Targeted delivery of compounds to *Trypanosoma brucei* using the melamine motif. Bioorganic & medicinal chemistry 17:2512–23

98.   Hunter L (2010) The C-F bond as a conformational tool in organic and biological chemistry. Beilstein journal of organic chemistry 6:38